

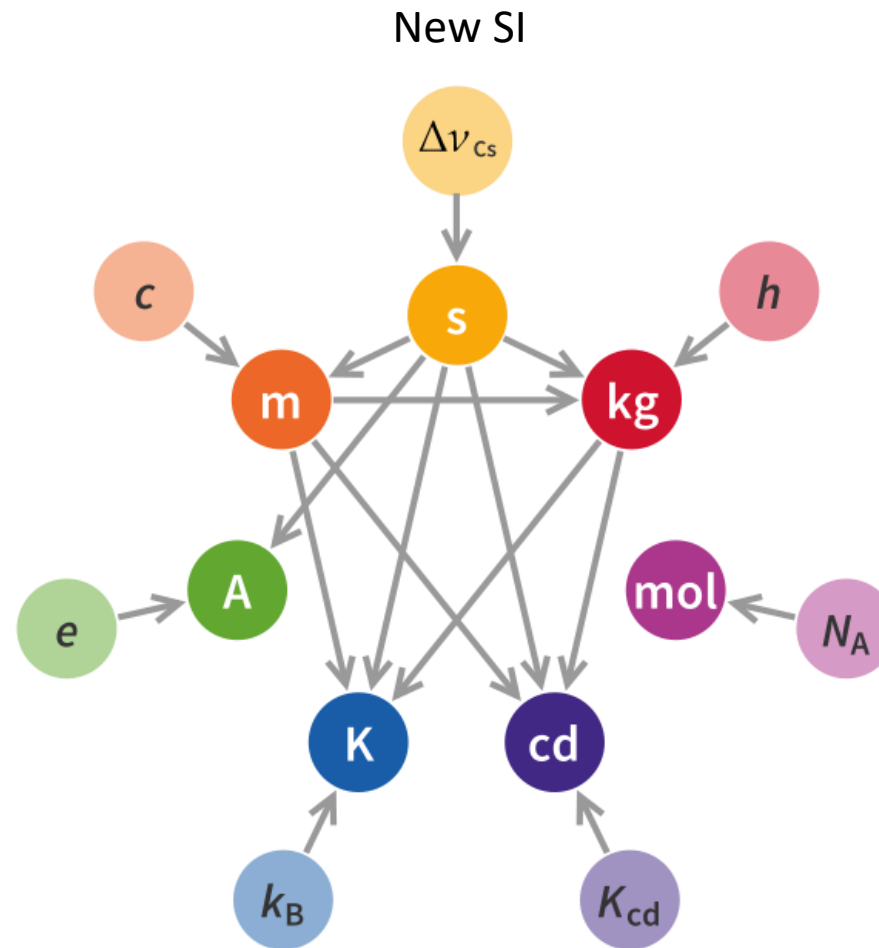
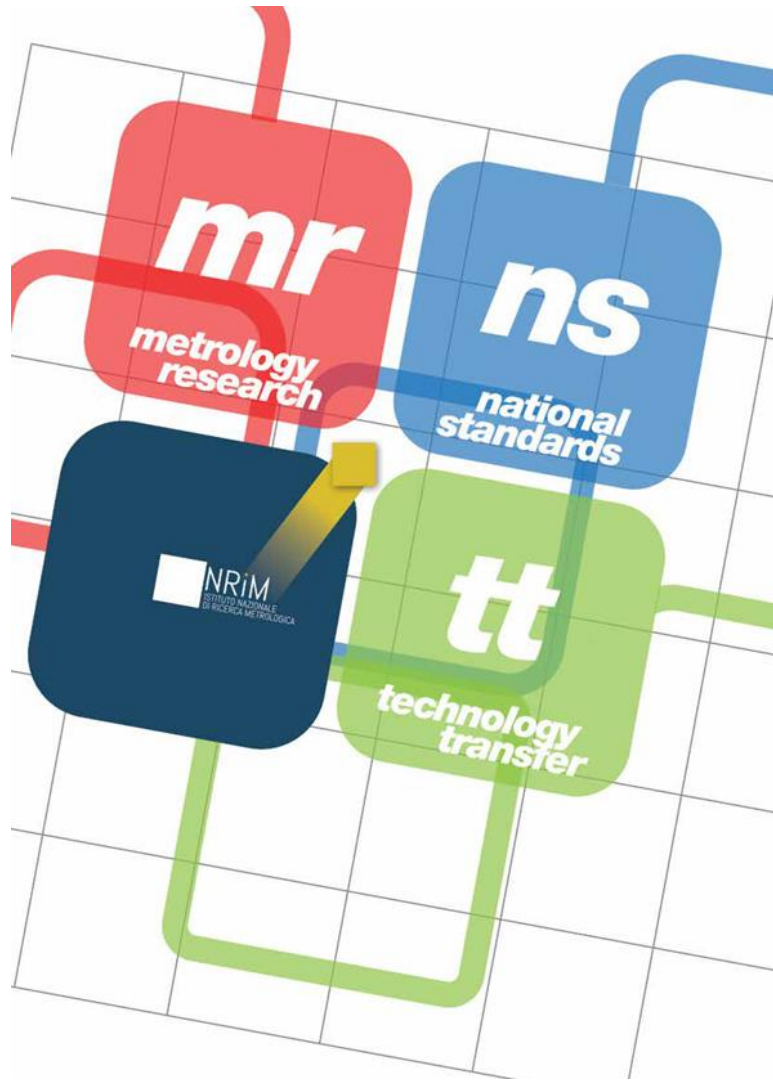


Josephson metamaterials: properties and fabrication

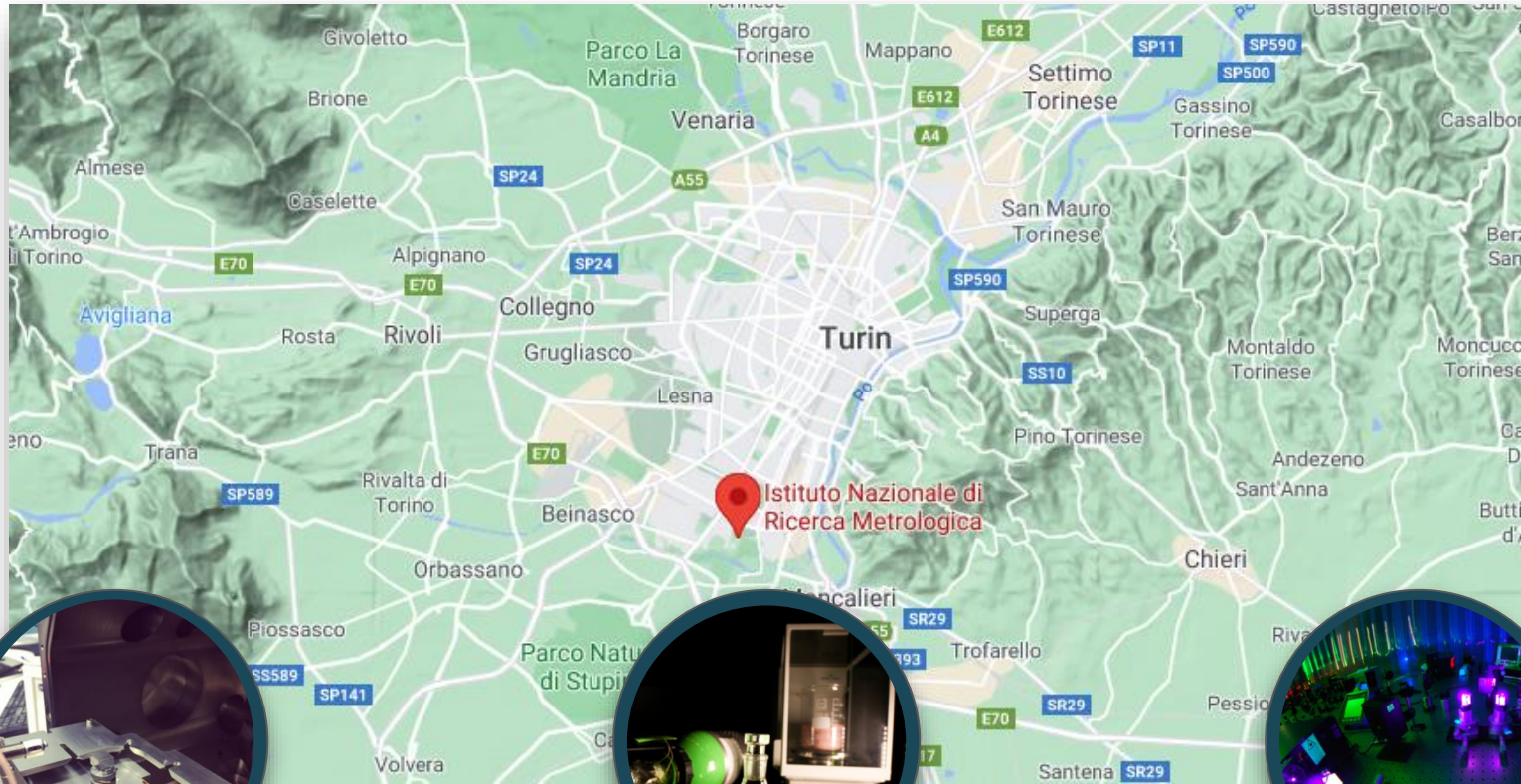
Circuit QED: from Quantum Devices to Analogues on Superconducting Circuits - Trento, October 3-5

Emanuele ENRICO

Introduction



Introduction



Advanced materials
metrology and life science

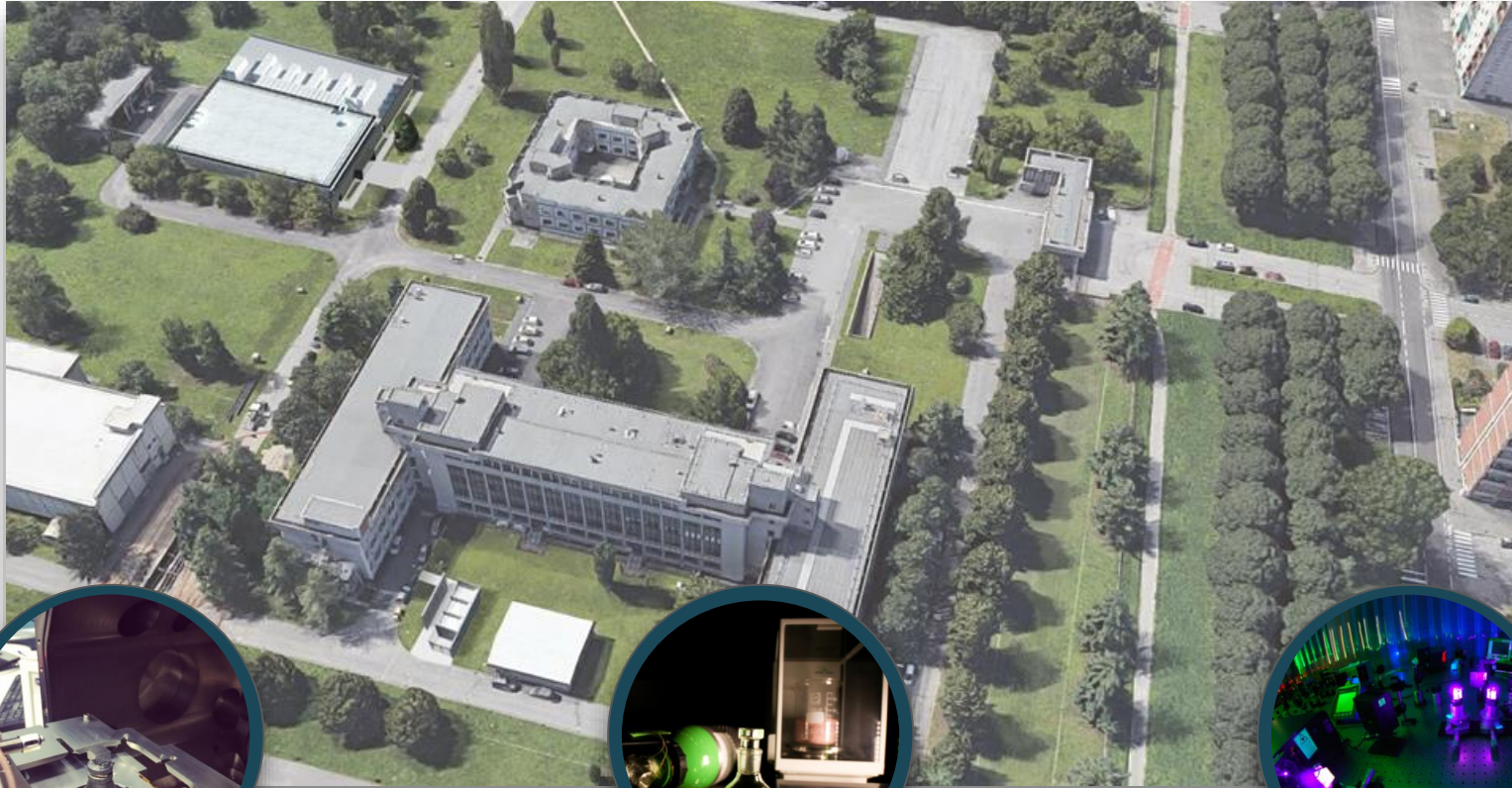


Applied metrology and
engineering



Quantum metrology and
nano technologies

Introduction

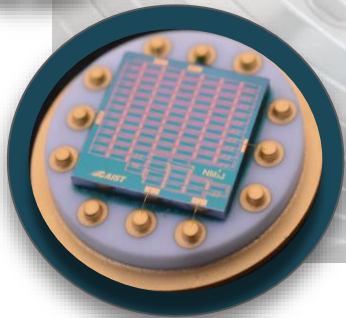


Advanced materials
metrology and life science

Applied metrology and
engineering

Quantum metrology and
nano technologies

Quantum Electronics - NanoTech

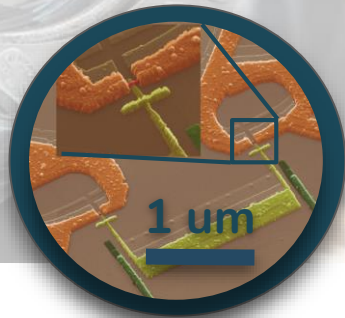


Quantum Hall Array
Resistance Standard

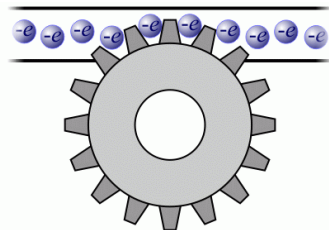
$$R_H = R_K/i$$

with $R_K = h/e^2$

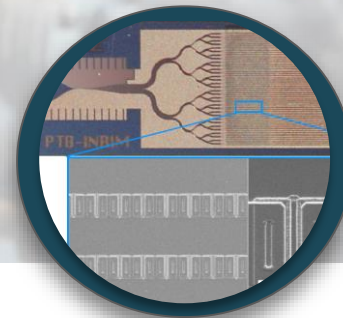
and $i = 1, 2, 3, 4, \dots$



Single-electron transistor low
DC current standard



$$I = nef$$

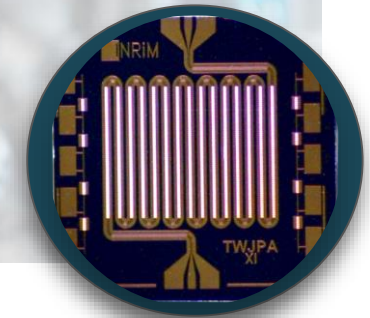


Josephson
Voltage Standard

$$V_J = n K_J f$$

with $K_J = h/2e$

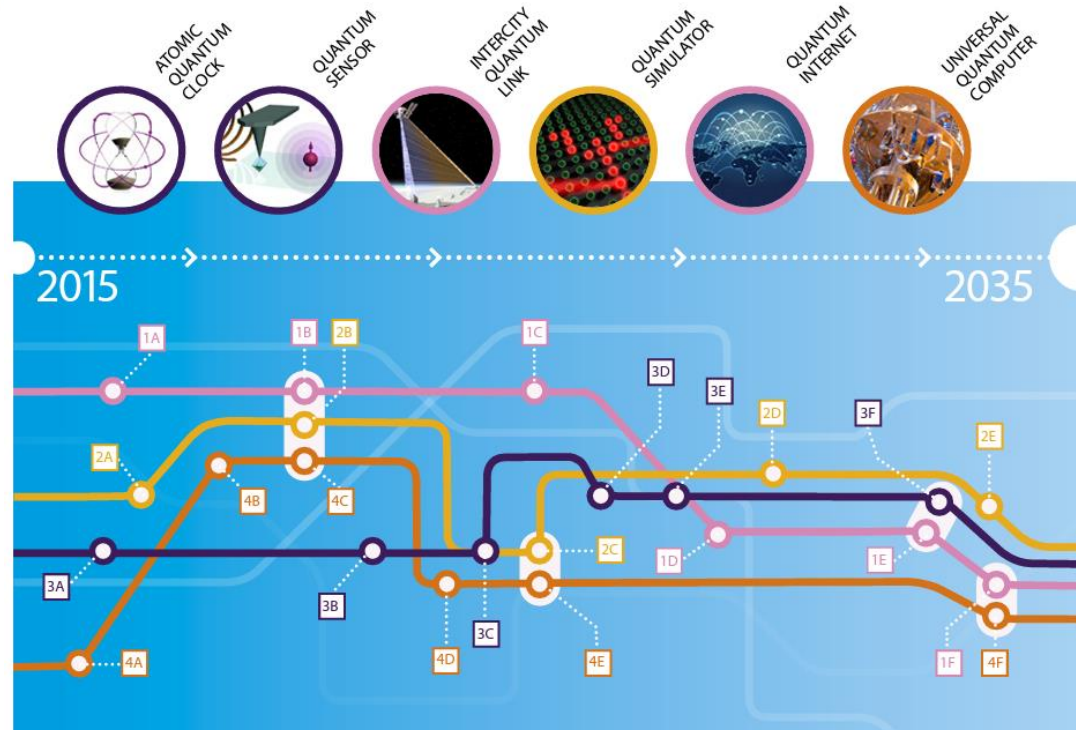
and $k = 1, 2, 3, 4, \dots$



Microwave photonics

| | |
|-------------------|--------------------------------------|
| ν | 1 GHz \rightarrow 20 GHz |
| $\lambda = c/\nu$ | 300 cm \rightarrow 15 cm |
| $E = h/\nu$ | 4 μ eV \rightarrow 80 μ eV |
| $T = E/k_B$ | 50 mK \rightarrow 1K |

Quantum Electronics - Applications



Pillars share **quantum states** experimental access, evidence and advantage

1. Communication

0 – 5 years

- A Core technology of quantum repeaters
- B Secure point-to-point quantum links

5 – 10 years

- C Quantum networks between distant cities
- D Quantum credit cards

> 10 years

- E Quantum repeaters with cryptography and eavesdropping detection
- F Secure Europe-wide internet merging quantum and classical communication

2. Simulators

- A Simulator of motion of electrons in materials
- B New algorithms for quantum simulators and networks

- C Development and design of new complex materials
- D Versatile simulator of quantum magnetism and electricity

- E Simulators of quantum dynamics and chemical reaction mechanisms to support drug design

3. Sensors

- A Quantum sensors for niche applications (incl. gravity and magnetic sensors for health care, geosurvey and security)
- B More precise atomic clocks for synchronisation of future smart networks, incl. energy grids

- C Quantum sensors for larger volume applications including automotive, construction
- D Handheld quantum navigation devices

- E Gravity imaging devices based on gravity sensors
- F Integrate quantum sensors with consumer applications including mobile devices

4. Computers

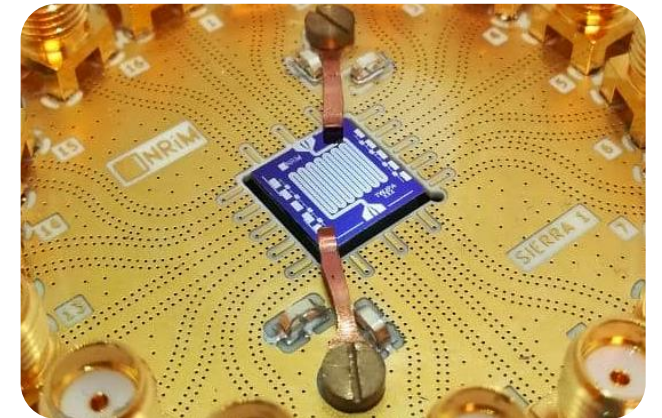
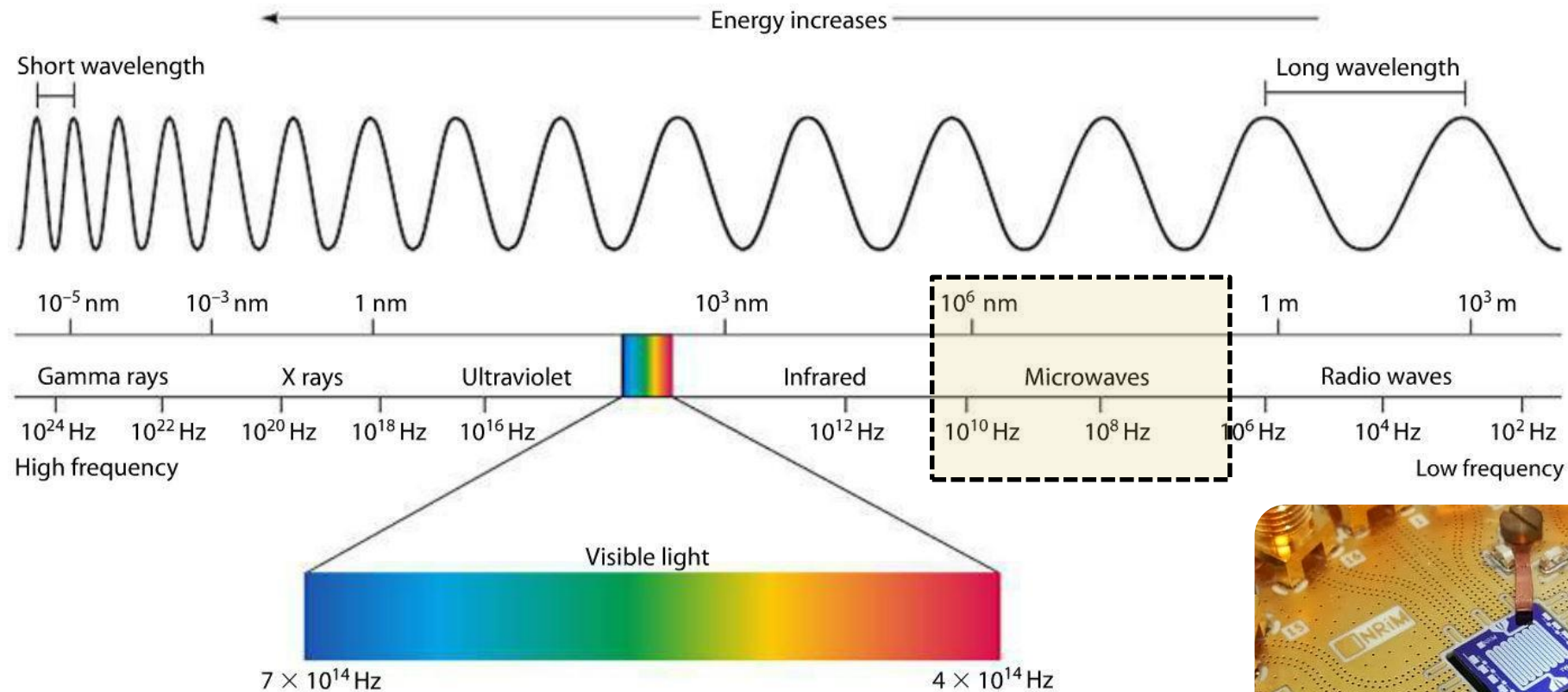
- A Operation of a logical qubit protected by error correction or topologically
- B New algorithms for quantum computers
- C Small quantum processor executing technologically relevant algorithms

- D Solving chemistry and materials science problems with special purpose quantum computer > 100 physical qubit

- E Integration of quantum circuit and cryogenic classical control hardware
- F General purpose quantum computers exceed computational power of classical computers

Quantum Manifesto, A New Era of Technology
May 2016

Quantum states – Energy scale



Circuit QED gives access to the **tuneability** of quantum states interactions with **chip-scale** technologies

Metrology perspective and current status of cQED related quantities

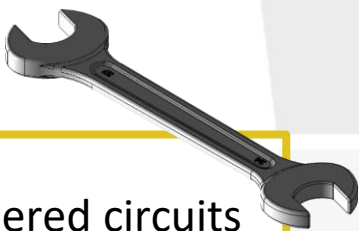
| Quantity | Traceability protocols | Calibration Standards | Uncertainty budget |
|-------------------------|------------------------|-----------------------|--------------------|
| <i>Temperature</i> | | | |
| <i>Frequency</i> | | | |
| <i>Voltage</i> | | | |
| <i>Current</i> | | | |
| <i>Impedance</i> | | | |
| <i>S-parameters</i> | | | |
| <i>Gain/Attenuation</i> | | | |
| <i>Power</i> | | | |

Circuit QED Toolbox

- Transmission lines
- Resonators / Cavities
- Qubits
- Isolators / Circulators
- Bias-tee
- Directional couplers
- Quantum limited linear amplifiers
- Detectors (transducers or counters eg. single microwave photon detectors)
- Nonclassical radiation sources

Circuit QED Toolbox

- Transmission lines
- Resonators / Cavities
- Qubits
- Isolators / Circulators
- Bias-tee
- Directional couplers
- Quantum limited linear amplifiers
- Detectors (transducers or counters eg. single microwave photon detectors)
- Nonclassical radiation sources



Josephson metamaterials are engineered circuits characterized by mixing processes promoting:

- Parametric amplification
Quantum limited added-noise
- Parametric downconversion
Nonclassical radiation

Nonlinear (meta) materials

Dipole electric momentum of a nonlinear material under electromagnetic stimulus

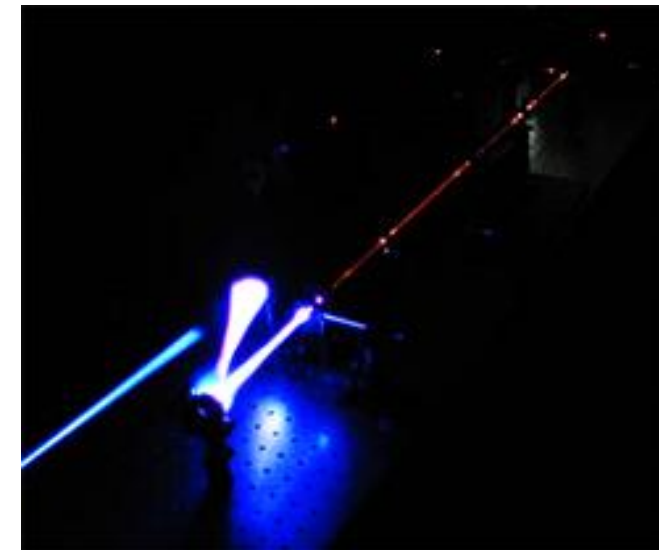
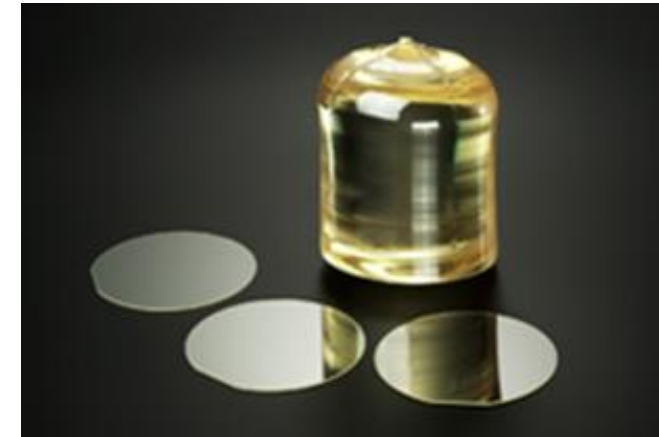
$$P(t) = \epsilon_0 (\chi^{(1)}E(t) + \chi^{(2)}E^2(t) + \chi^{(3)}E^3(t) + \dots)$$

When a (weak) signal is pumped by a (strong) one

$$E(t) = E_p \cos(\omega_p t) + E_s \cos(\omega_s t)$$

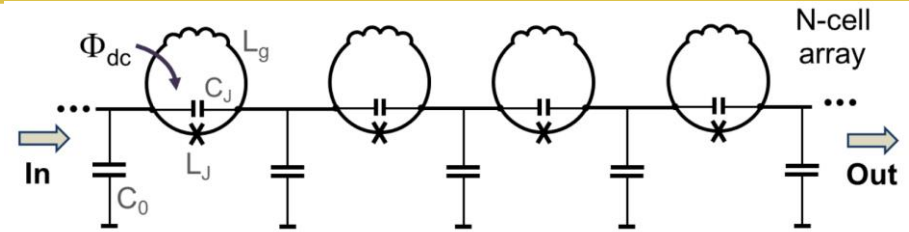
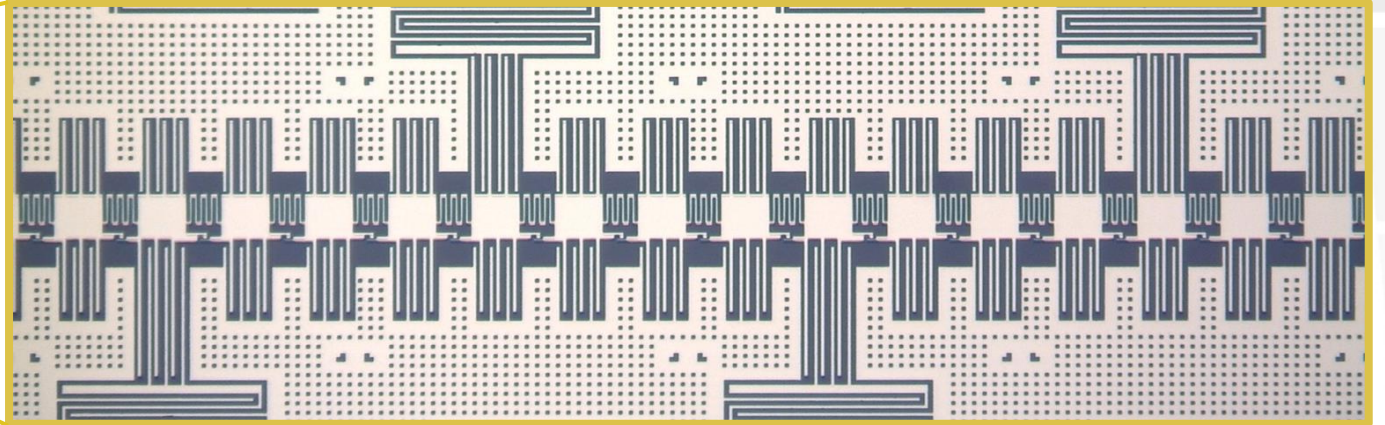
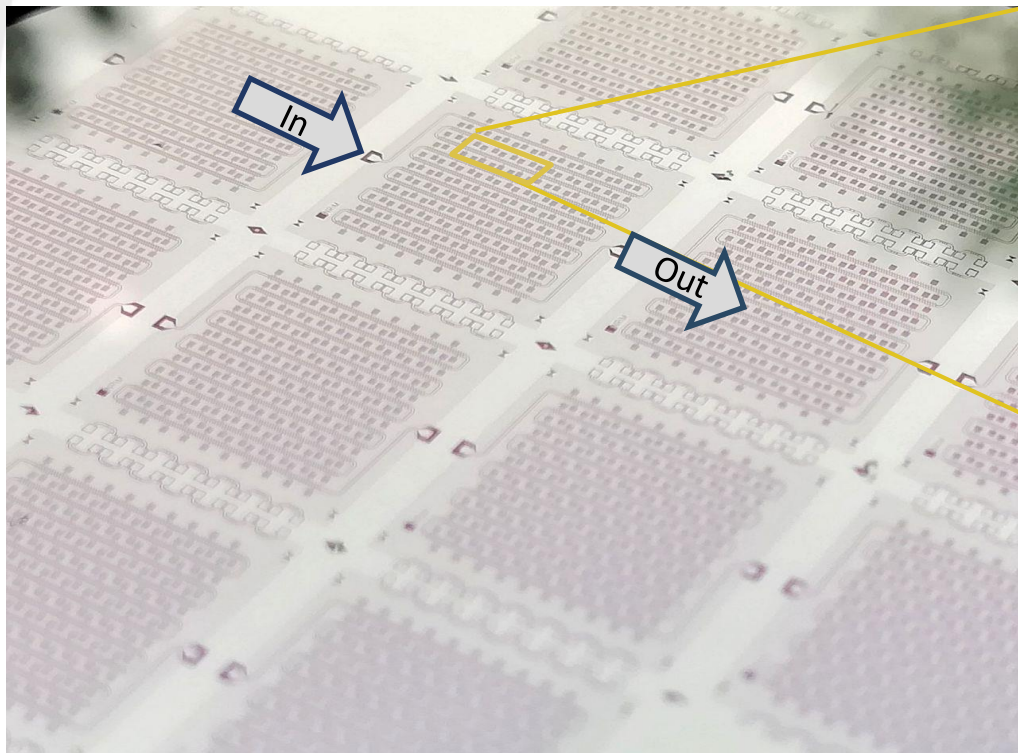
It generates

- Second harmonics (SHG)
- Sum frequency
- Different frequency or Parametric Down Conversion (PDC)

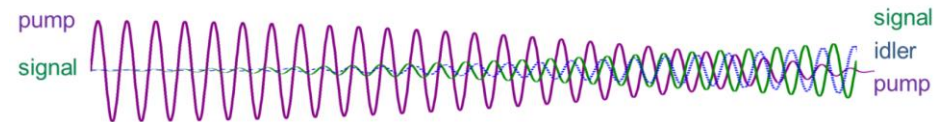


Nonlinear (meta) materials - μ Waves

- Transmission line (eg. CPW or stripline) + **identical** meta-atom (with JJ nonlinearity)
- Effects of the interaction with the single cell are perturbative -> avoid abrupt changes that acts like point defects or scattering sites (crystal analogy)



Very small phase mismatch \Rightarrow almost **exponential gain**, $\sqrt{G} \propto e^{gN}$



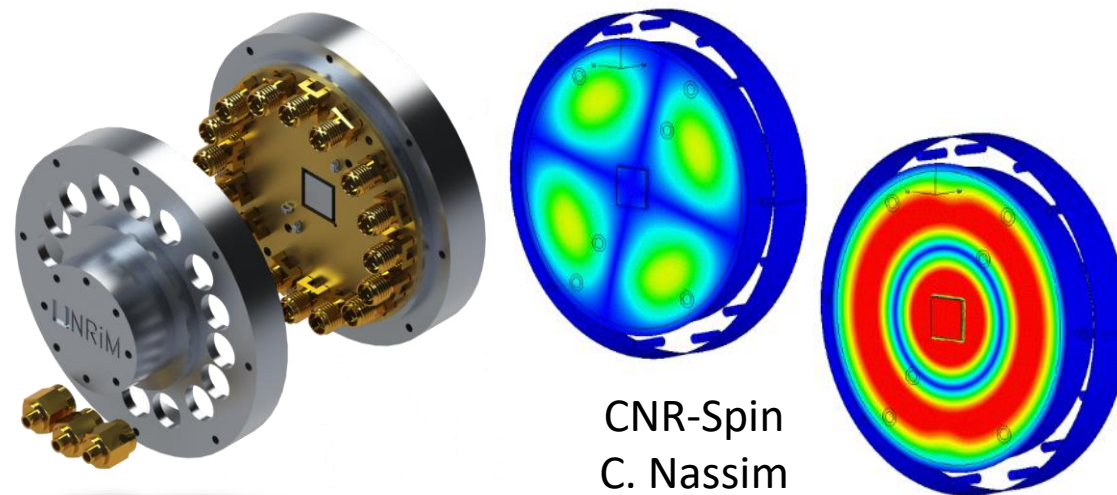
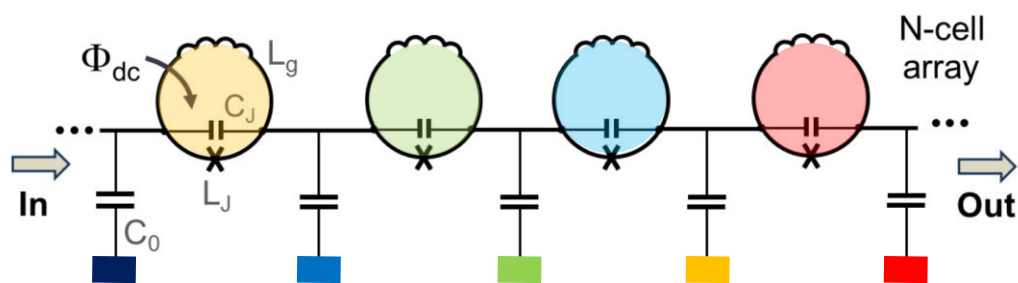
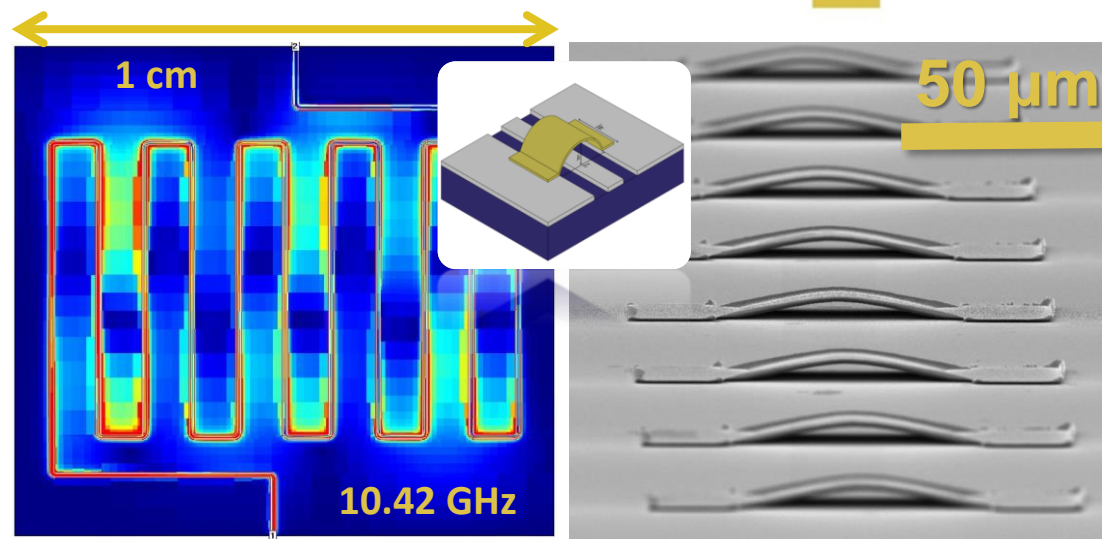
S. Pagano et al., *Development of Quantum Limited Superconducting Amplifiers for Advanced Detection*, IEEE Trans. Appl. Supercond, **32**, 4 (2022)

Zorin, *Phys. Rev. Appl.* **6**, 034006 (2016)

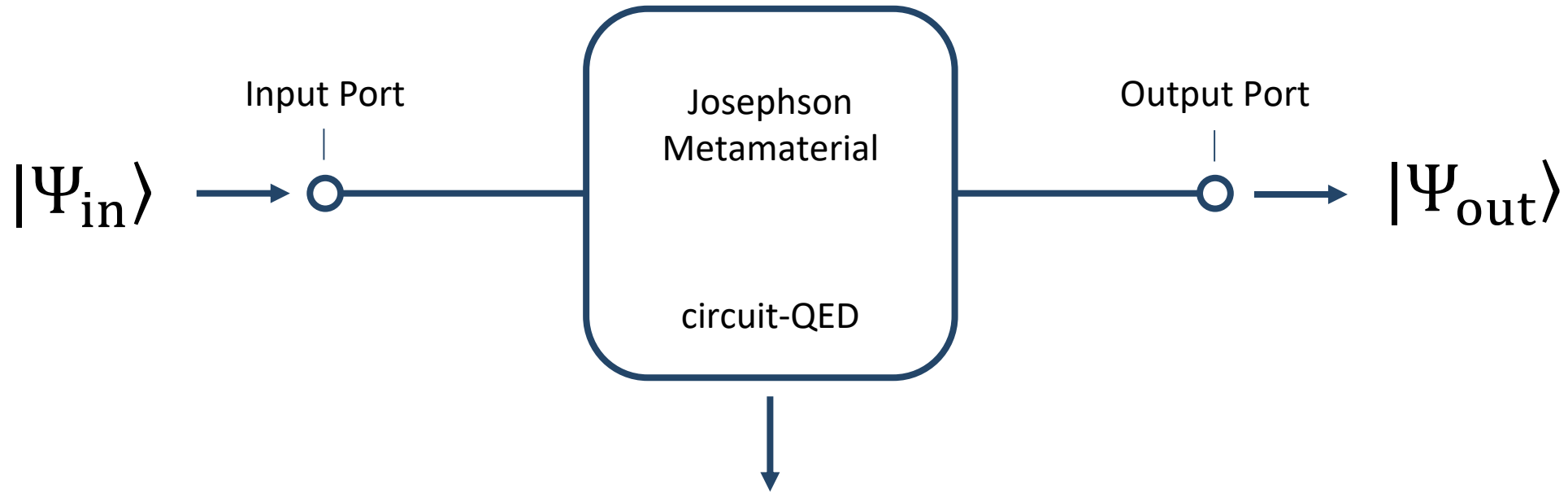


Transmission lines peculiarities

- Packed CPW/stripline
- Influenced by substrate/dielectrics choice
materials losses (eg. TLS)
- Total size vs. chip size
slotline modes -> Airbridges
- Chip and connectors size influence packaging
cavity modes



Modelling



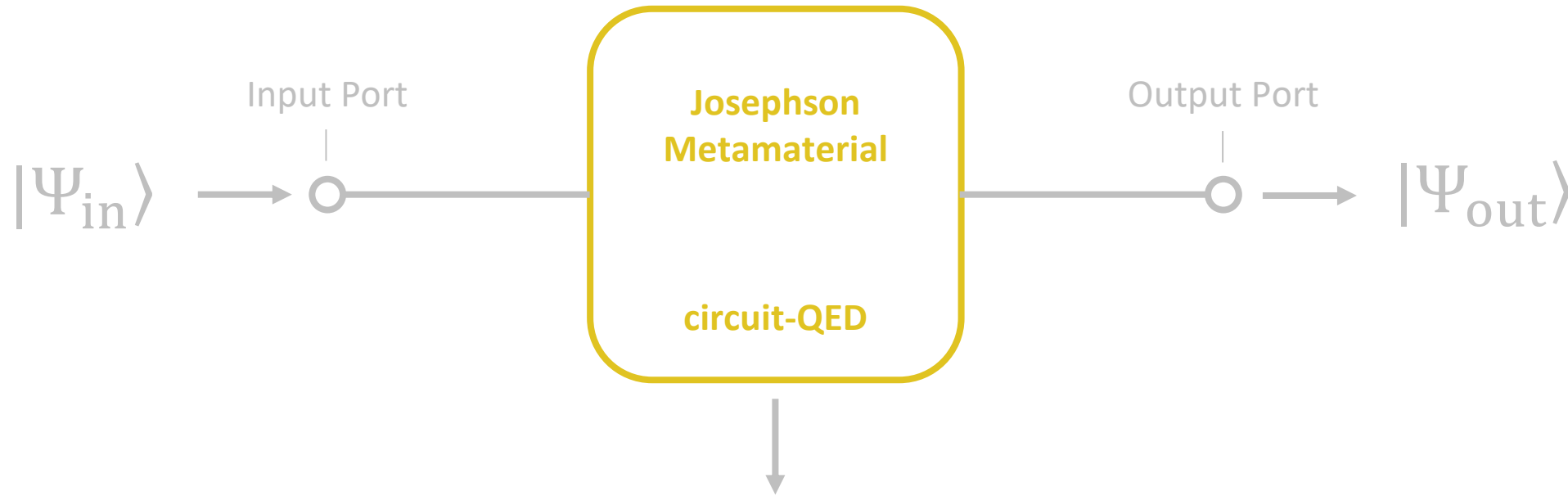
Classic observables:

- Gain
- Noise Figure
- Noise Temperature

Quantum behavior:

- Occupancy probability distribution

Modelling



Classic observables:

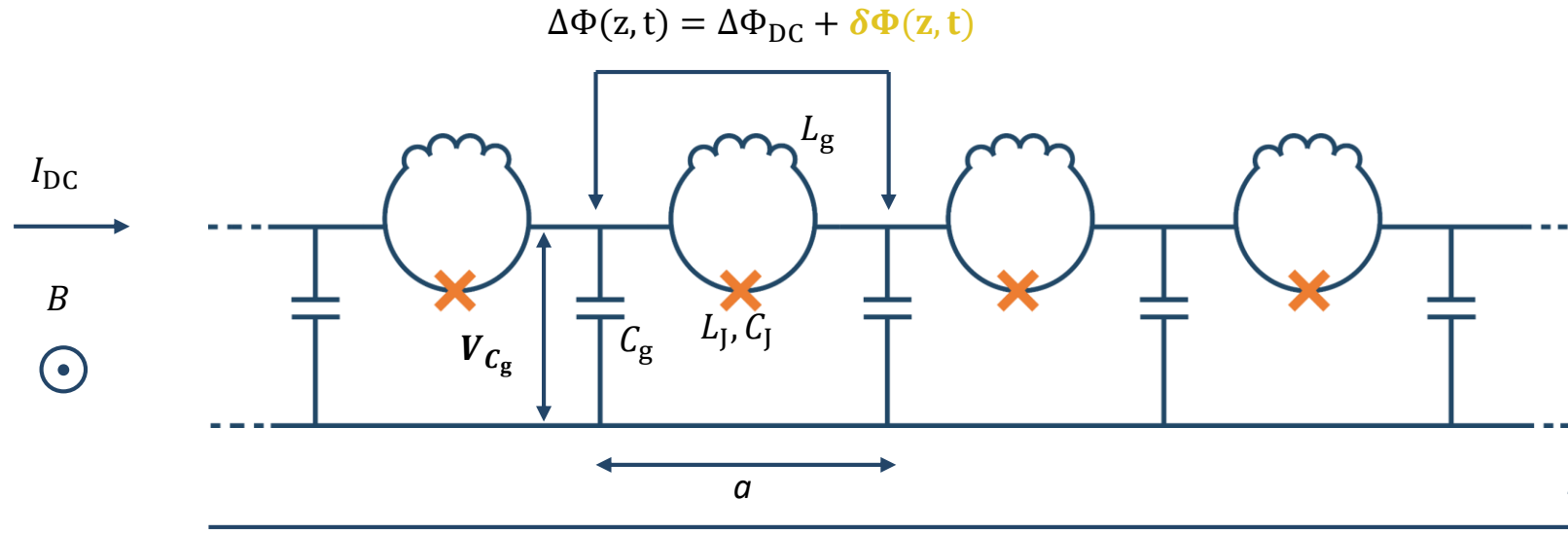
- Gain
- Noise Figure
- Noise Temperature

Quantum behavior:

- Occupancy probability distribution

First Quantization Hamiltonian

We adapt and further extend the work presented in [1] to an **rf-SQUID based Josephson Traveling Wave Parametric Amplifier** [2]



$\Delta\Phi_{DC}$ is the **constant** flux difference due to external bias

$\delta\Phi(z, t)$ is the **time-dependent** flux difference induced by the travelling waves

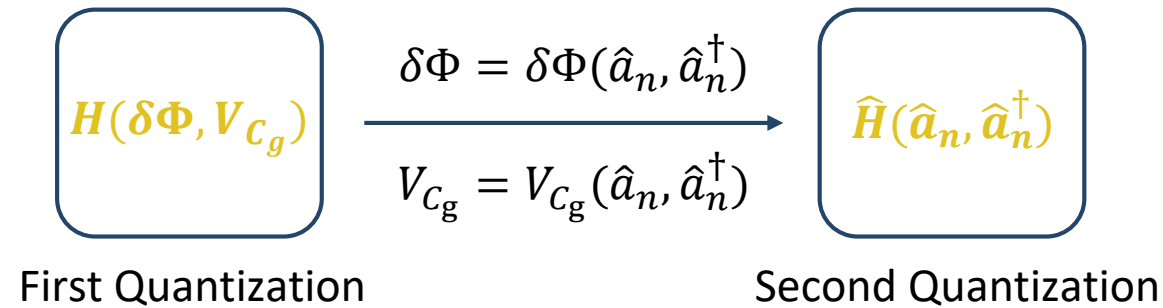
The **first quantization Hamiltonian** can be written as the sum of the electromagnetic energy stored in each component of the transmission line

$$H = \frac{1}{a} \int_0^{aN} \left[\frac{1}{2L_g} \Delta\Phi(z, t)^2 + \varphi_0 I_c \left(1 - \cos\left(\frac{\Delta\Phi(z, t)}{\varphi_0}\right) \right) + \frac{C_J}{2} \left(\frac{\partial \Delta\Phi(z, t)}{\partial t} \right)^2 + \frac{C_g}{2} V_{C_g}^2(z, t) \right] dz$$

[1] T. H. A. van der Reep, "Mesoscopic Hamiltonian for Josephson traveling-wave parametric amplifier", Phys. Rev. A **99**, 063838 (2019)

[2] A. B. Zorin, "Josephson Traveling-Wave Parametric Amplifier with Three-Wave Mixing", Phys. Rev. App. **6**, 034006 (2016)

Second Quantization Hamiltonian



Second Quantization Hamiltonian

The Hamiltonian describes all the **energy preserving interactions** between 3 or 4 traveling waves (i.e., the **parametric down conversion**, the **sum frequency generation**, the **high order harmonics generation**, etc..)

$$H = \hbar\chi_0 + \sum_n \hbar\chi_1^{(n)} \left(\hat{a}_n^\dagger \hat{a}_n + \frac{1}{2} \right) + \sum_{n,l,m} \hbar\chi_3^{(n,l,m)} \{ \hat{a} + \hat{a}^\dagger \}_{n,l,m} \cdot \delta_{\Delta_{n,l,m},0} + \sum_{n,l,m,s} \hbar\chi_4^{(n,l,m,s)} \{ \hat{a} + \hat{a}^\dagger \}_{n,l,m,s} \cdot \delta_{\Delta_{n,l,m,s},0}$$

Energy from **external bias**

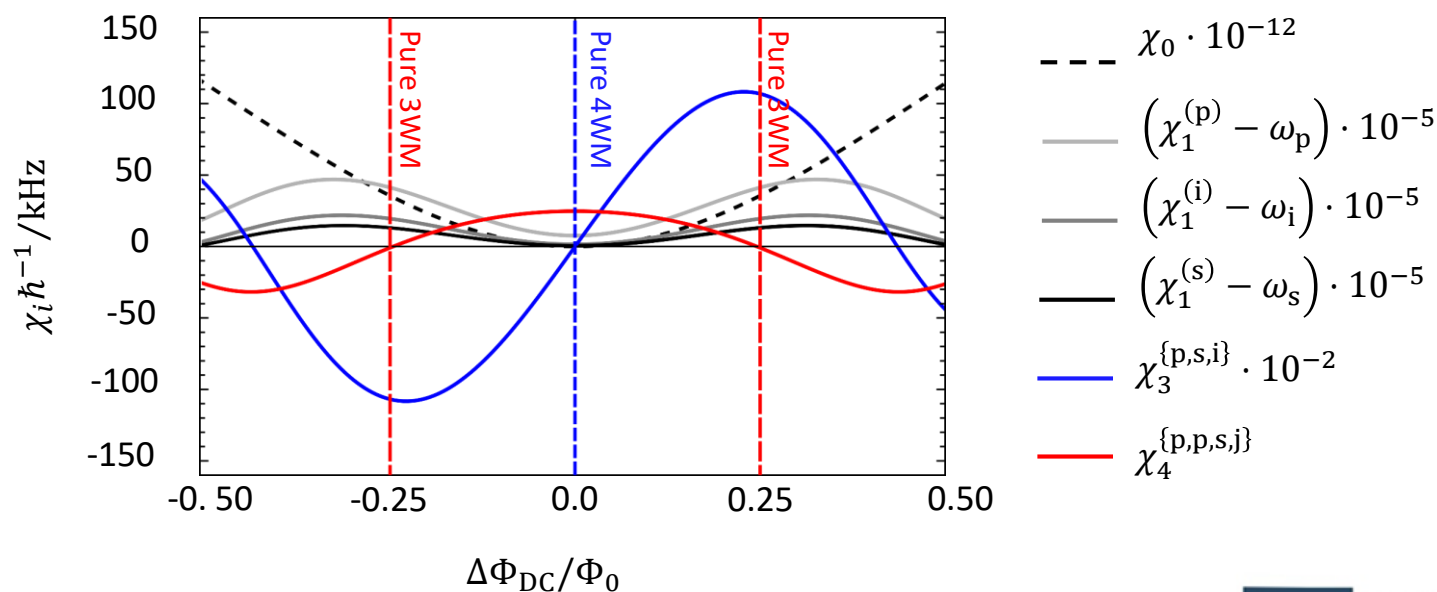
Energy of the **propagating waves**

All 3-wave mixing energy-preserving processes

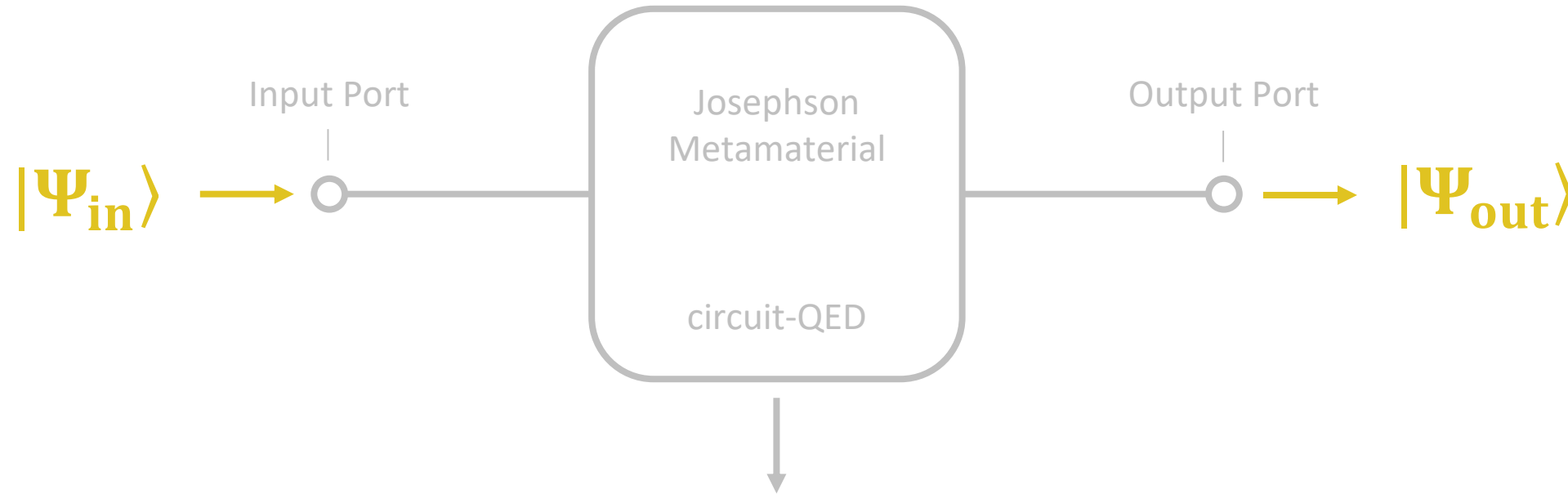
All 4-wave mixing energy-preserving processes

For **parametric down-conversion**

- **3WM** $n, l, m = \{p, s, i\}$
with $\omega_p = \omega_s + \omega_i$
- **4WM** $n, l, m, s = \{p, s, j\}$
with $2\omega_p = \omega_s + \omega_j$



Quantum states evolution



Classic observables:

- Gain
- Noise Figure
- Noise Temperature

Quantum behavior:

- Occupancy probability distribution

CMEs from Heisenberg Equation

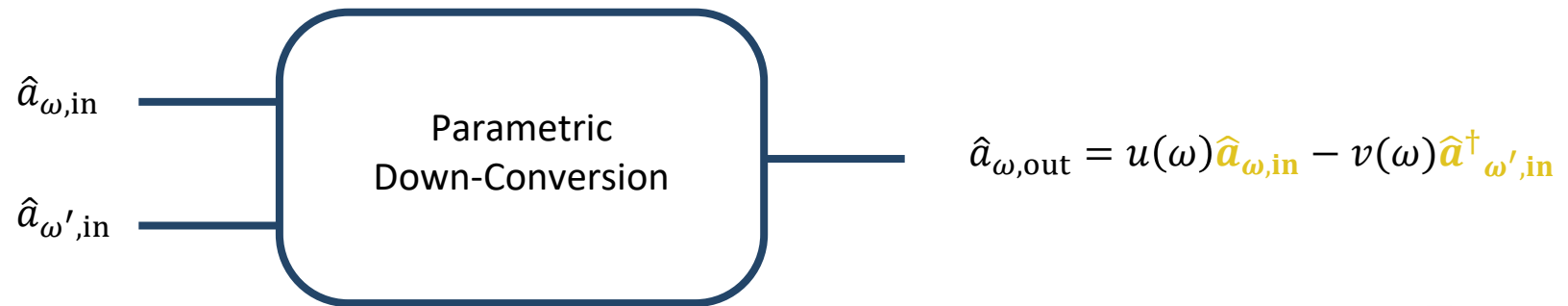
Selecting a proper bias condition, the amplifier can work as a pure 3-Wave Mixer or 4-Wave Mixer (H_{3WM} , H_{4WM}). In this condition the **evolution of propagating modes** can be derived solving the **Heisenberg equation**:

$$\frac{d\hat{a}_n}{dt} = \frac{i}{\hbar} [H_{3WM(4WM)}, \hat{a}_n] + \frac{\partial \hat{a}_n}{\partial t} \quad \text{where } n = \{p, s, i, j\}$$

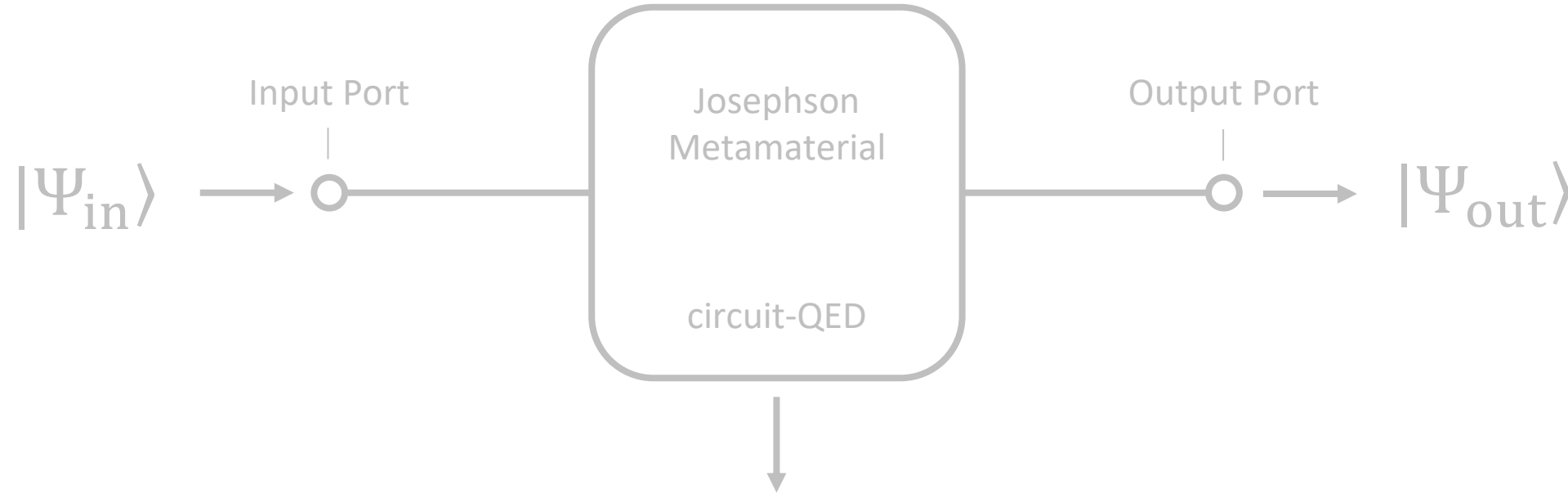
Under the **undepleted and classical pump** approximation, the output field at the **signal frequency ω** is:

$$\hat{a}_\omega(t) = \left[\left(\cosh(gt) + \frac{i\Psi}{2g} \sinh(gt) \right) \hat{a}_{\omega, \text{in}} - \left(\frac{iY}{g} \sinh(gt) \right) \hat{a}_{\omega', \text{in}}^\dagger \right] e^{-i\left(\frac{\Psi}{2}\right)t}$$

where g is the **complex gain factor**, Ψ is the **density phase mismatch** and Y is the **interaction parameter**.



Classical quantities



Classic observables:

- **Gain**
- **Noise Figure**
- **Noise Temperature**

Quantum behavior:

- Occupancy probability distribution

Signal photon number at output

$$\langle \hat{n}_{\omega, out} \rangle = \langle \hat{a}_{\omega, out}^\dagger \hat{a}_{\omega, out} \rangle =$$

$$= |u(\omega)|^2 \langle \hat{n}_{\omega, in} \rangle + |v(\omega)|^2 \langle \hat{n}_{\omega', in} \rangle + i \left(u^*(\omega) v(\omega) \langle \hat{a}_{\omega, in}^\dagger \hat{a}_{\omega', in}^\dagger \rangle - u(\omega) v^*(\omega) \langle \hat{a}_{\omega', in} \hat{a}_{\omega, in} \rangle \right) + |v(\omega)|^2$$

Amplification of the input field at ω frequency

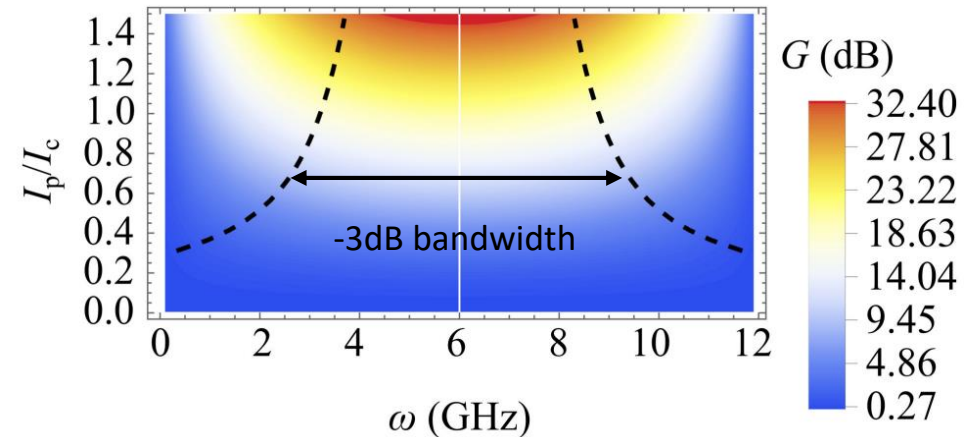
Contribution from the **spontaneous annihilation** of a pump photon

Added noise photons ($\langle \text{vac} | \hat{n}_{\omega, out} | \text{vac} \rangle$)

Contribution to the amplification of the **input field at ω** frequency due to the presence of an input signal at **ω' frequency**

Contribution from the **spontaneous creation** of a pump photon

$$G(\omega) \equiv \frac{\langle \hat{n}_{\omega, out} \rangle}{\langle \hat{n}_{\omega, in} \rangle} = |u(\omega)|^2$$



Noise figure and Signal to Noise Ratio

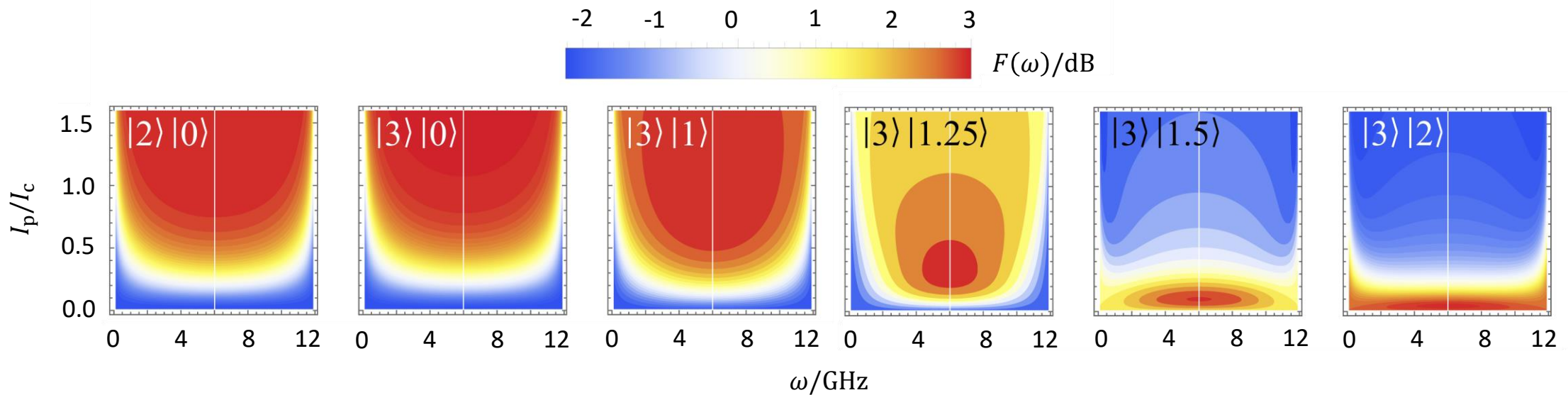
$$F(\omega) \equiv \frac{\text{SNR}_{\text{in}}(\omega)}{\text{SNR}_{\text{out}}(\omega)}$$

$$\text{SNR}_{\text{in}}(\omega) \equiv \frac{\langle \hat{n}_{\omega,\text{in}} \rangle^2}{\langle (\Delta \hat{n}_{\omega,\text{in}})^2 \rangle}$$

$$\text{SNR}_{\text{out}}(\omega) \equiv \frac{\langle \hat{n}_{\omega,\text{out}} \rangle^2 - \langle \hat{n}_{\omega,\text{out}}^{\text{vac}} \rangle^2}{\langle (\Delta \hat{n}_{\omega,\text{out}})^2 \rangle} \quad [4]$$

└ Variance of the input/output photon number ┘

Supposing at the input a **Bimodal Coherent state**: $|\Psi_C\rangle = D(\alpha_\omega)|0_\omega\rangle D(\alpha_{\omega'})|0_{\omega'}\rangle = |\alpha_\omega\rangle|\alpha_{\omega'}\rangle$



An **idler** tone at the input port **influences the Noise figure** $F(\omega)$ of the amplifier

[4] Z. Shi *et al.*, "Quantum noise properties of non-ideal optical amplifiers and attenuators", *J. Opt.* **13** (2011)

Noise Temperature

The **effective temperature** $T_{\text{eff}}(\omega)$ of the amplifier is the temperature that a **Bose-Einstein distribution** should have to equal the output ω mode occupancy generated by a vacuum input state [5]:

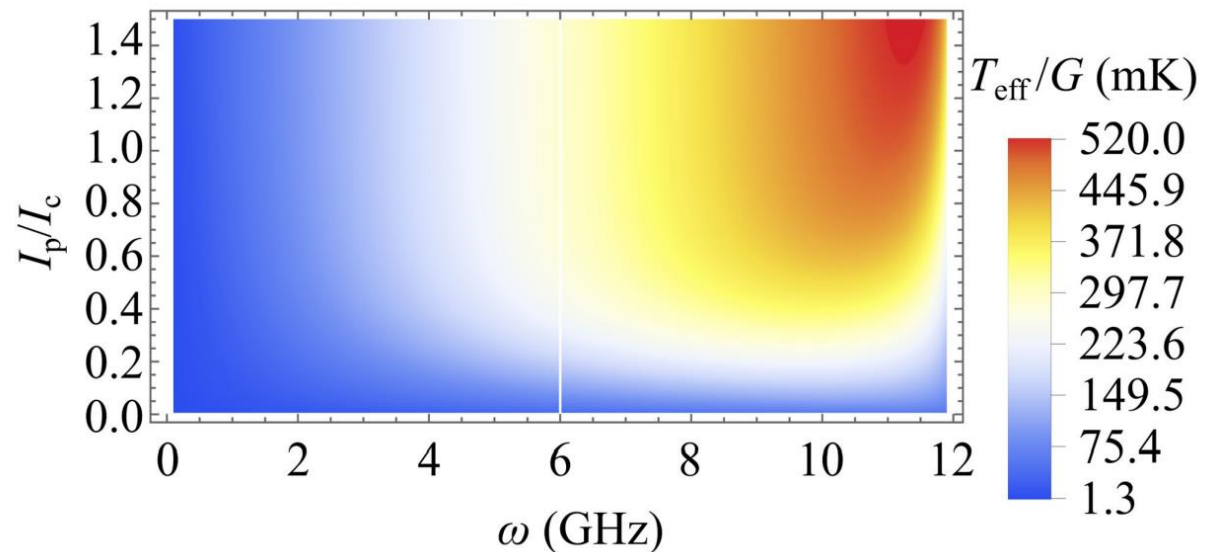
$$\frac{1}{e^{\hbar\omega/k_B T_{\text{eff}}(\omega)} - 1} = |v(\omega)|^2$$

The **noise temperature** $T_n(\omega)$ is the effective temperature normalized on the gain minus the contribution given by the fluctuation of the input vacuum state:

$$T_n(\omega) = \frac{T_{\text{eff}}(\omega)}{G(\omega)} - \frac{1}{2} \frac{\hbar\omega}{k_B}$$

For high gain $T_n(\omega)$ approaches the **Standard Quantum Limit**:

$$T_{n,\text{SQL}} = \frac{1}{2} \frac{\hbar\omega}{k_B}$$

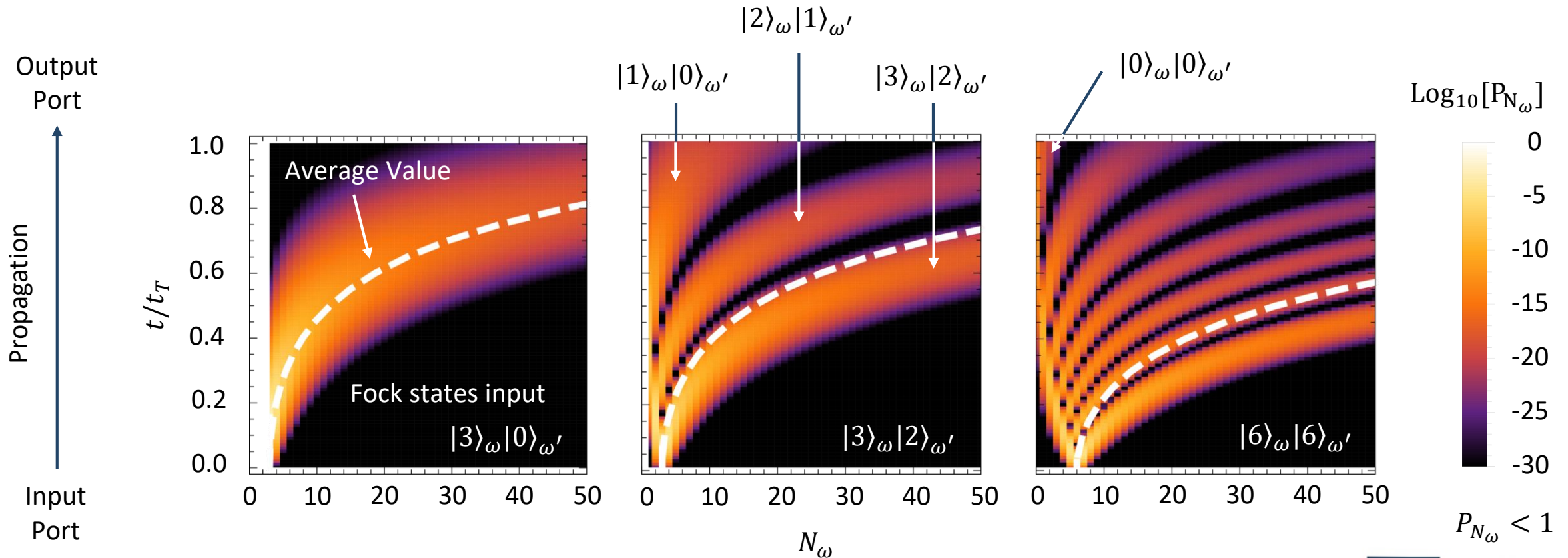


[5] A. A. Clerk *et al.*, "Introduction to quantum noise, measurement, and amplification", *Rev. Mod. Phys.* **82**, 1155 (2010)

Time-evolution of bimodal Fock states

The average photon number at frequency ω at a certain time t can be written in terms of the **probability** P_{N_ω} to find N_ω photons at a given time

$$\langle n_\omega(t) \rangle = \sum_{N_\omega} P_{N_\omega}(t) \cdot N_\omega$$



For more details ...

PHYSICAL REVIEW B **104**, 184517 (2021)

Quantum model for rf-SQUID-based metamaterials enabling three-wave mixing and four-wave mixing traveling-wave parametric amplification

Angelo Greco and Luca Fasolo

INRiM, Istituto Nazionale di Ricerca Metrologica, Strada delle Cacce 91, 10135 Torino, Italy
and Department of Electronics and Telecommunications, PoliTo, Corso Castellfardo 39, 10129 Torino, Italy

Alice Meda and Luca Callegaro

INRiM, Istituto Nazionale di Ricerca Metrologica, Strada delle Cacce 91, 10135 Torino, Italy

Emanuele Enrico

INRiM, Istituto Nazionale di Ricerca Metrologica, Strada delle Cacce 91, 10135 Torino, Italy
and INFN, Trento Institute for Fundamental Physics and Applications, I-38123 Povo, Trento, Italy

(Received 30 April 2021; revised 22 October 2021; accepted 25 October 2021; published 24 November 2021)

A quantum model for Josephson-based metamaterials working in the three-wave mixing (3WM) and four-wave mixing (4WM) regimes at the single-photon level is presented. The transmission line taken into account, namely Josephson traveling wave parametric amplifier (JTWPA), is a bipole composed of a chain of rf-SQUIDs, which can be biased by a DC current or a magnetic field to activate the 3WM or 4WM nonlinearities. The model exploits a Hamiltonian approach to analytically determine the time evolution of the system both in the Heisenberg and interaction pictures. The former returns the analytic form of the gain of the amplifier, while the latter allows recovering the probability distributions vs time of the photonic populations. The model is applied to Fock and coherent input states. The dependence of the metamaterial's nonlinearities on the circuit parameters in a lumped model framework while evaluating the effects of the model validity.

DOI: [10.1103/PhysRevB.104.184517](https://doi.org/10.1103/PhysRevB.104.184517)



A. Greco *et al.*, Phys. Rev. B (2021)

IEEE TRANSACTIONS ON APPLIED SUPERCONDUCTIVITY, VOL. 32, NO. 4, JUNE 2022

1700306

Bimodal Approach for Noise Figures of Merit Evaluation in Quantum-Limited Josephson Traveling Wave Parametric Amplifiers

L. Fasolo, C. Barone, M. Borghesi, G. Carapella, A. P. Caricato, I. Carusotto, W. Chung, A. Cian, D. Di Gioacchino, E. Enrico, P. Falferi, M. Faverzani, E. Ferri, G. Filatrella, C. Gatti, A. Giachero, D. Giubertoni, A. Greco, Ç. Kutlu, A. Leo, C. Ligi, P. Livreri, G. Maccarrone, B. Margesin, G. Maruccio, A. Matlashov, C. Mauro, R. Mezzena, A. G. Monteduro, A. Nucciotti, L. Oberto, S. Pagano, V. Pierro, L. Piersanti, M. Rajteri, A. Rettaroli, S. Rizzato, Y. K. Semertzidis, S. Uchaikin, and A. Vinante

Abstract—The advent of ultra-low noise microwave amplifiers revolutionized several research fields demanding quantum-limited technologies. Exploiting a theoretical bimodal description of a linear phase-preserving amplifier, in this contribution we analyze some of the intrinsic properties of a model architecture (i.e., an rf-SQUID based Josephson Traveling Wave Parametric Amplifier) in terms of amplification and noise generation for key case study input states (Fock and coherent). Furthermore, we present an analysis of the output signals generated by the parametric amplification mechanism when thermal noise fluctuations feed the device.

Index—microwave photonics, noise figure, superconducting quantum circuits.

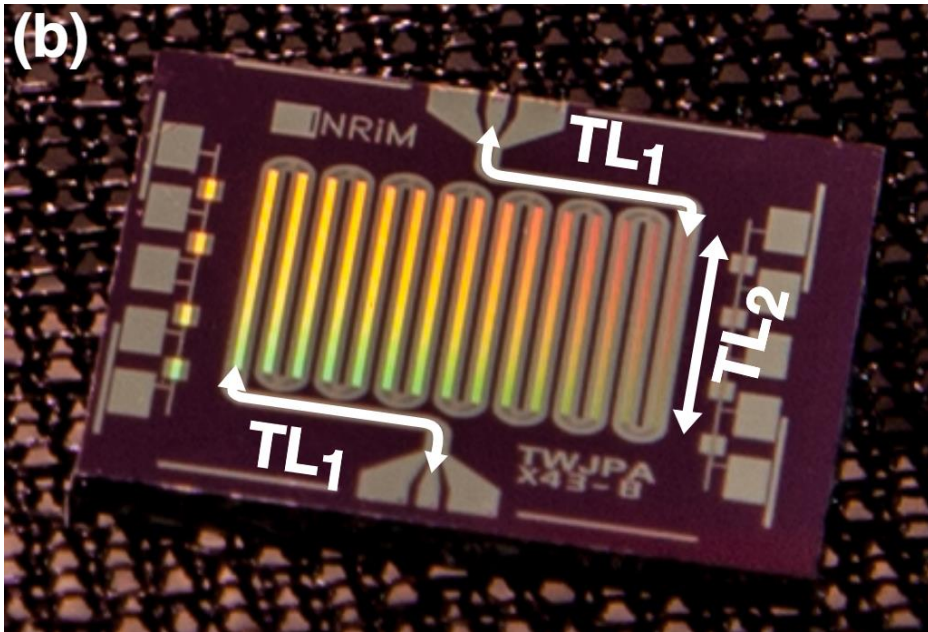


the amplifier is considered as a two-ports black-box driven at a pump frequency ω_p that amplifies a bosonic input mode at frequency ω . The amplification is associated with the creation of a second mode at frequency $\omega' = \omega_p - \omega$ (the so-called idler mode of a three-wave mixing parametric amplification [15]) that is commonly considered as an internal mode of the amplifier that causes the onset of noise at the output port. Here, we extend and give a different perspective of this description considering the case in which an uncorrelated idler mode is already present at the input port (i.e., considering a bimodal input field), analyzing the effect of the interaction between these modes inside the amplifier in terms of typical noise estimators. This operative condition may arise in real measurement setups where the amplifier is exploited, for instance, for the multiplexed readout of broadband signals [16] or for the joint detection and amplification of probing signals in a microwave quantum illumination

L. Fasolo *et al.*, IEEE TAS (2022)

Fabrication Example

JTWPA – DARTWARS Project

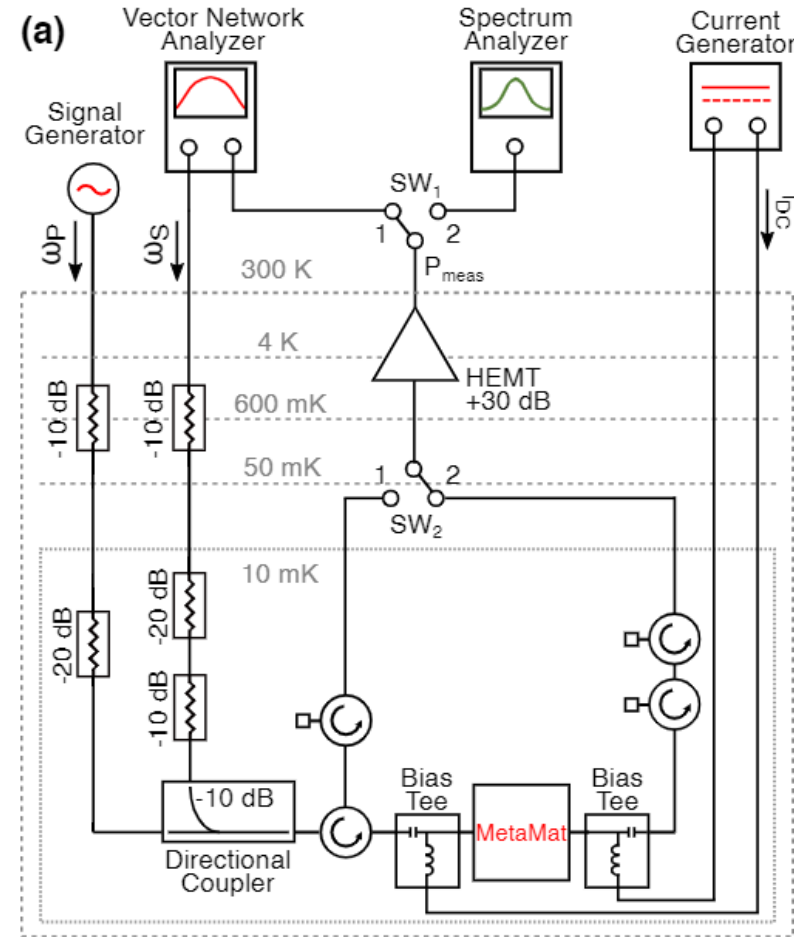
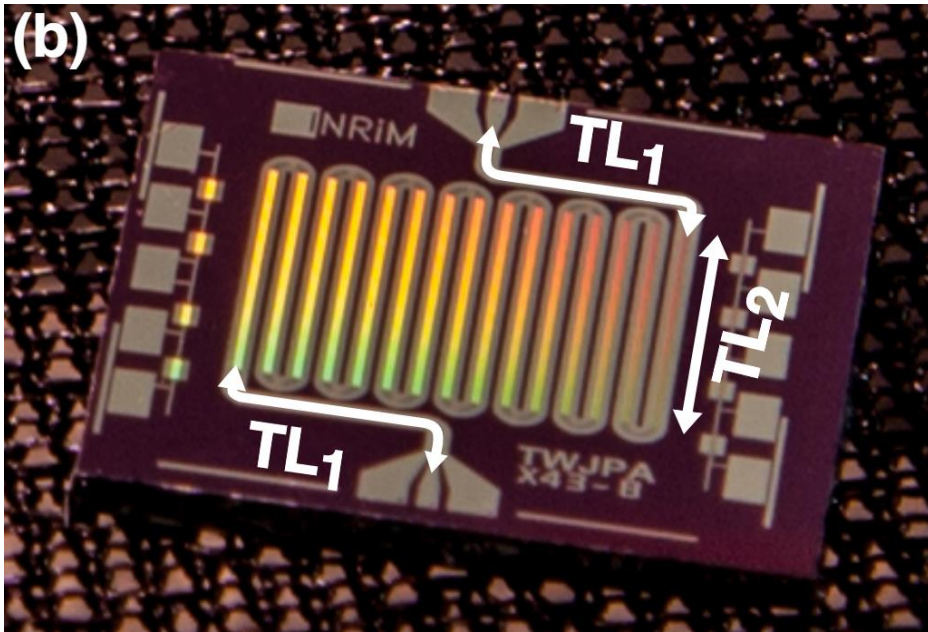
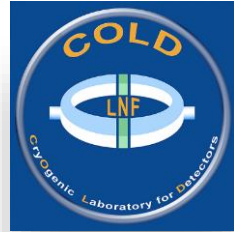


Preliminary samples

- Poor impedance matching of TL1, TL2 and 50Ω
- No dispersion engineering
- High Josephson Junctions parameters spread
- No slopline modes rejection techniques

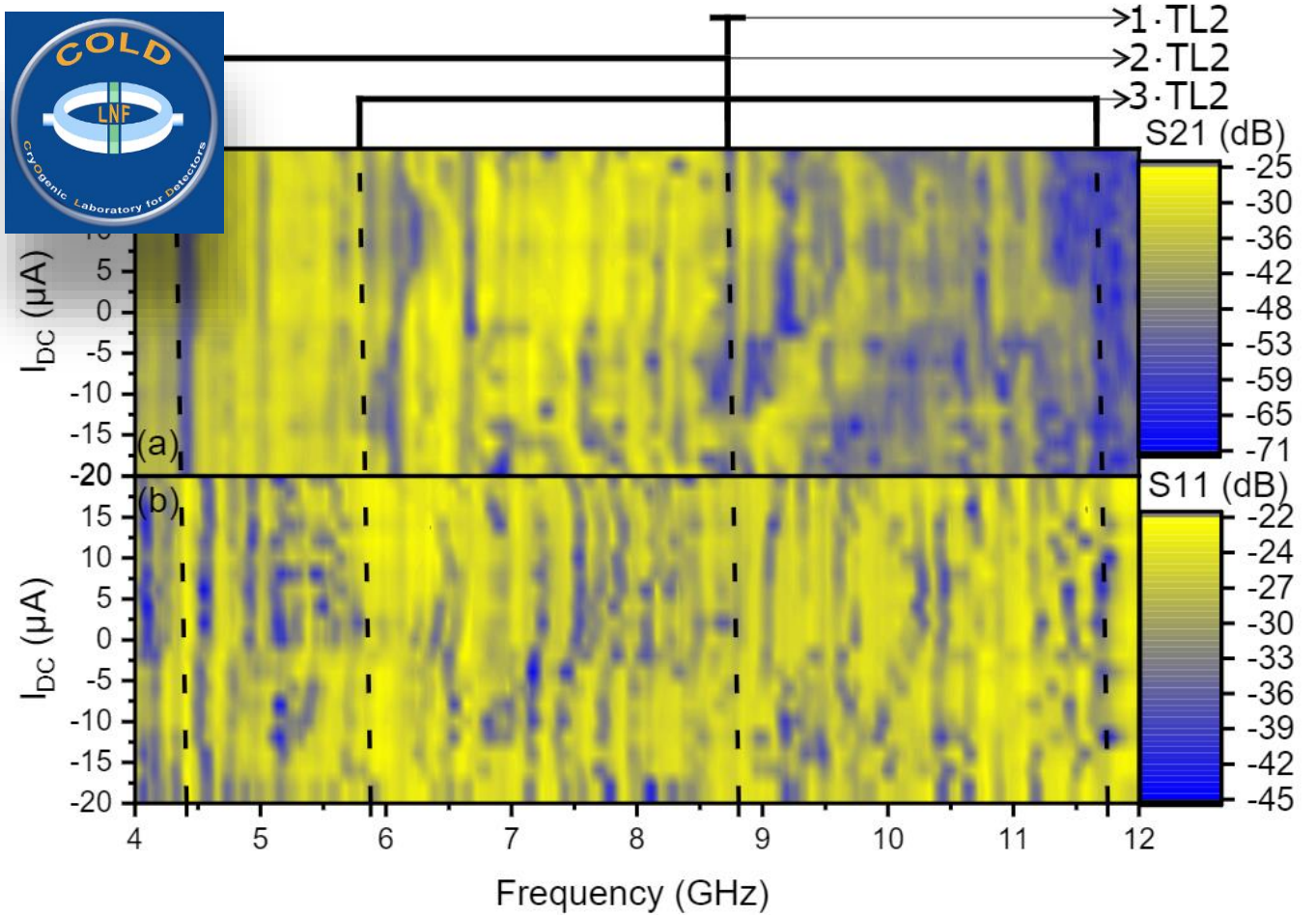
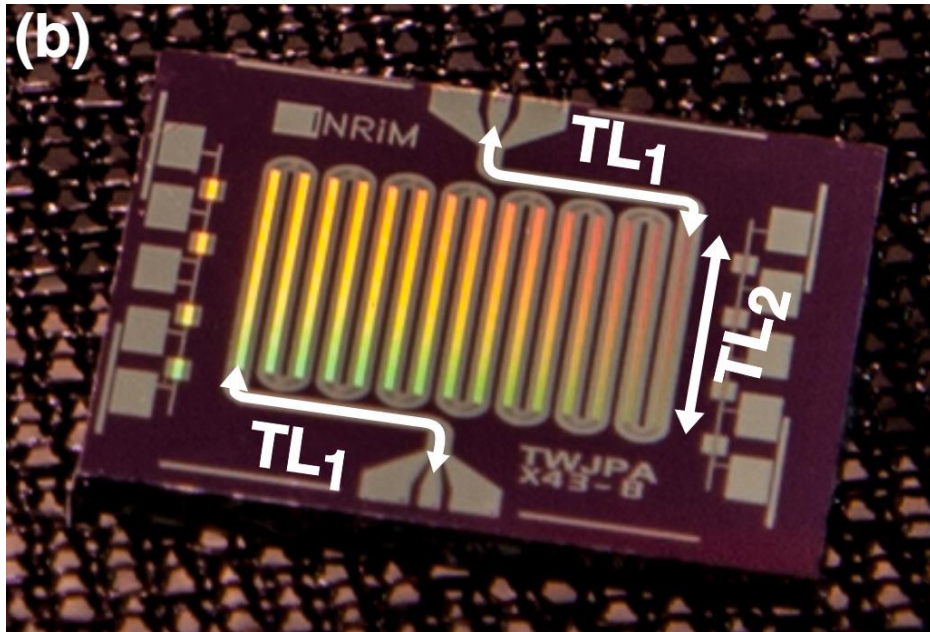
Fabrication Example

JTWPA – DARTWARS Project



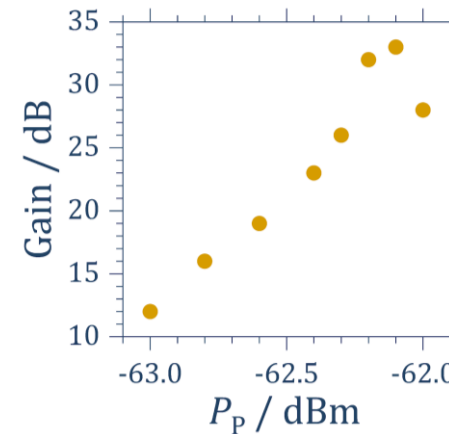
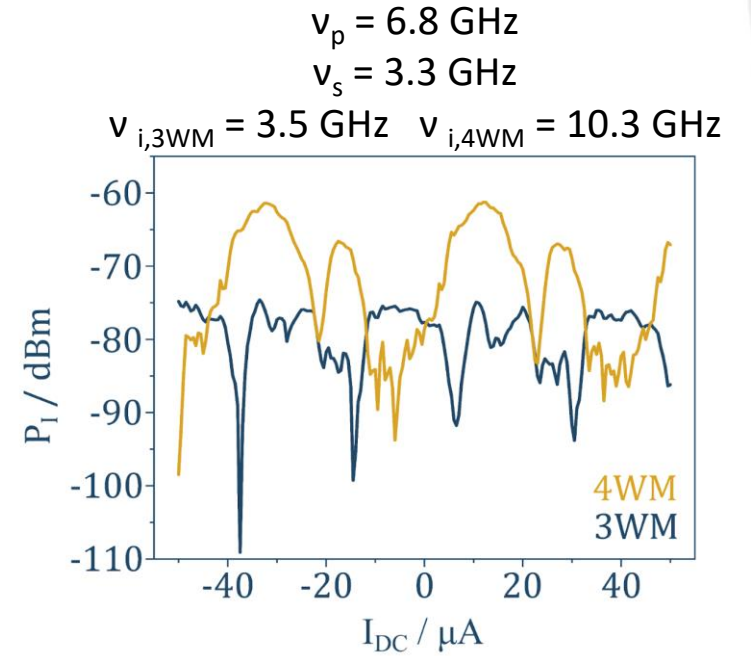
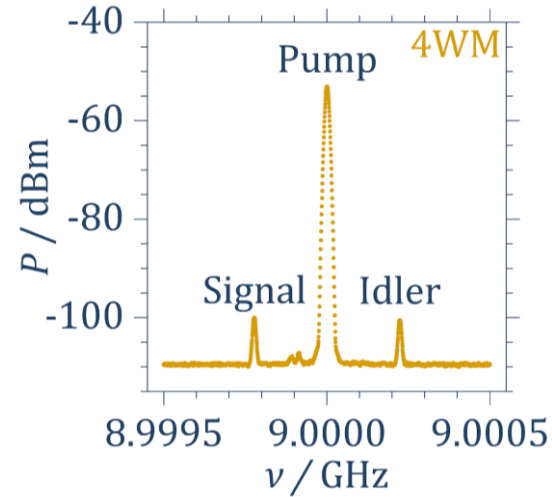
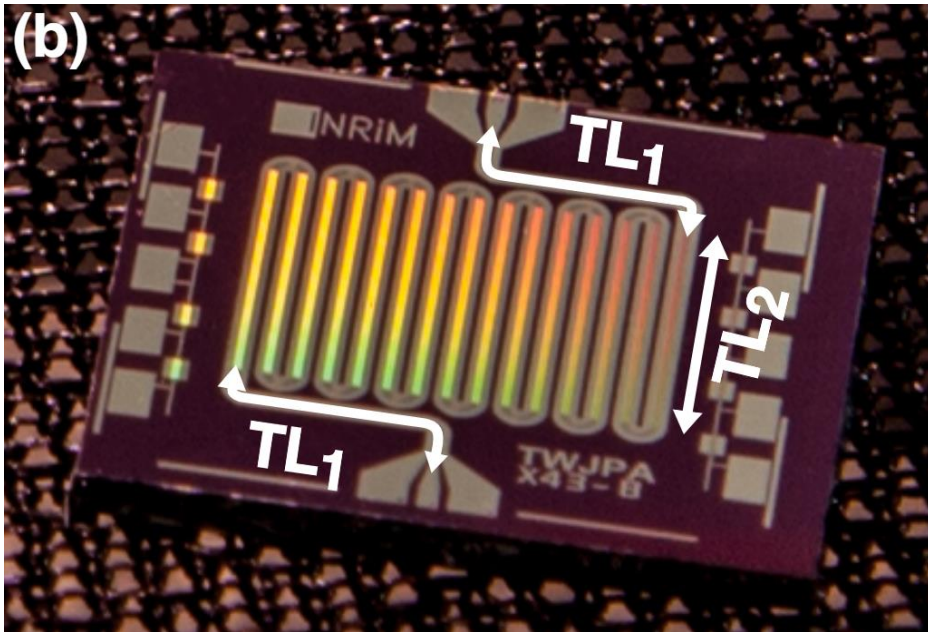
Fabrication Example

JTWPA – DARTWARS Project



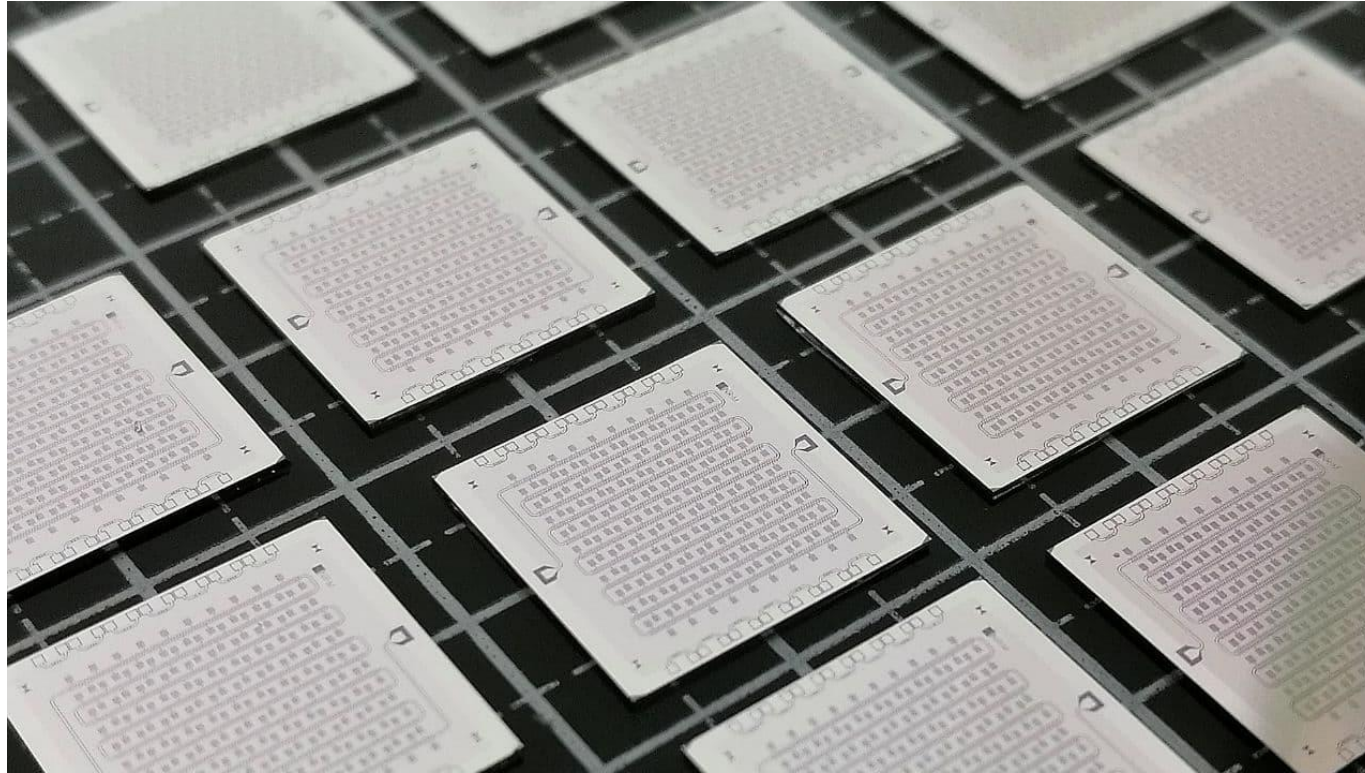
Fabrication Example

JTWPA – DARTWARS Project



Fabrication Example

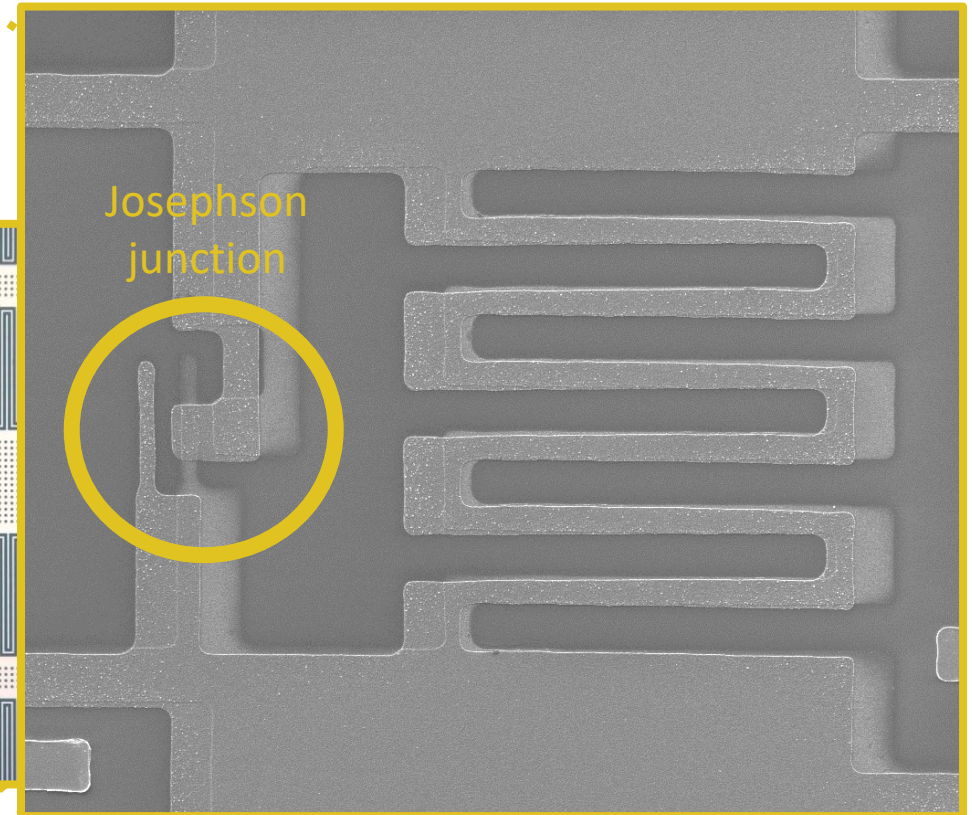
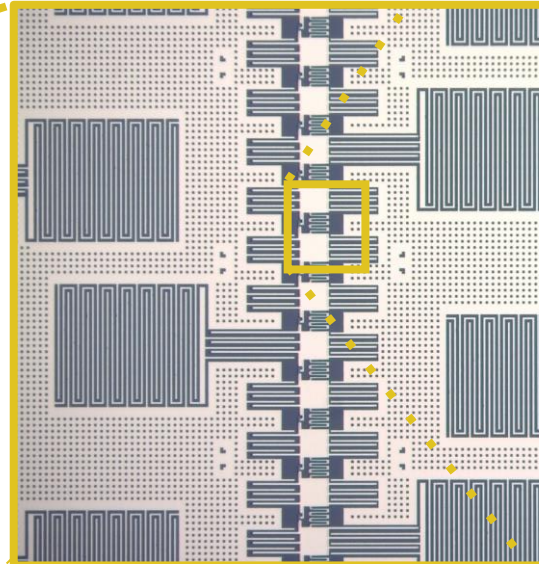
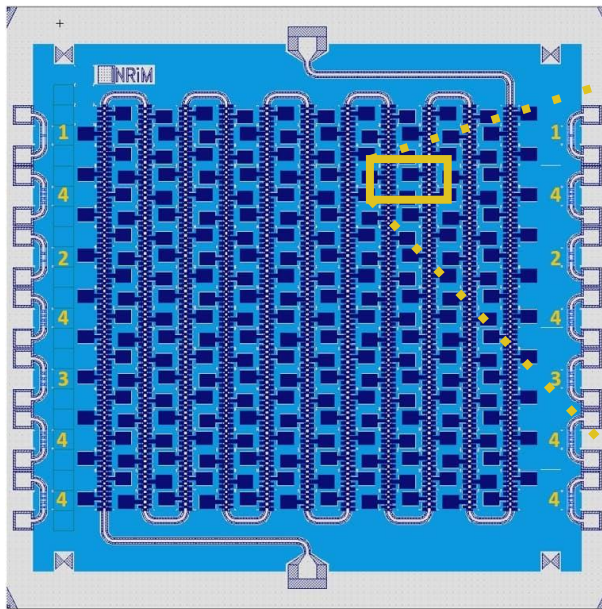
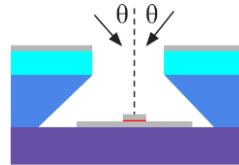
JTWPA – DARTWARS Project



Fabrication Example

JTWPA – DARTWARS Project

Conventional double angle evaporation

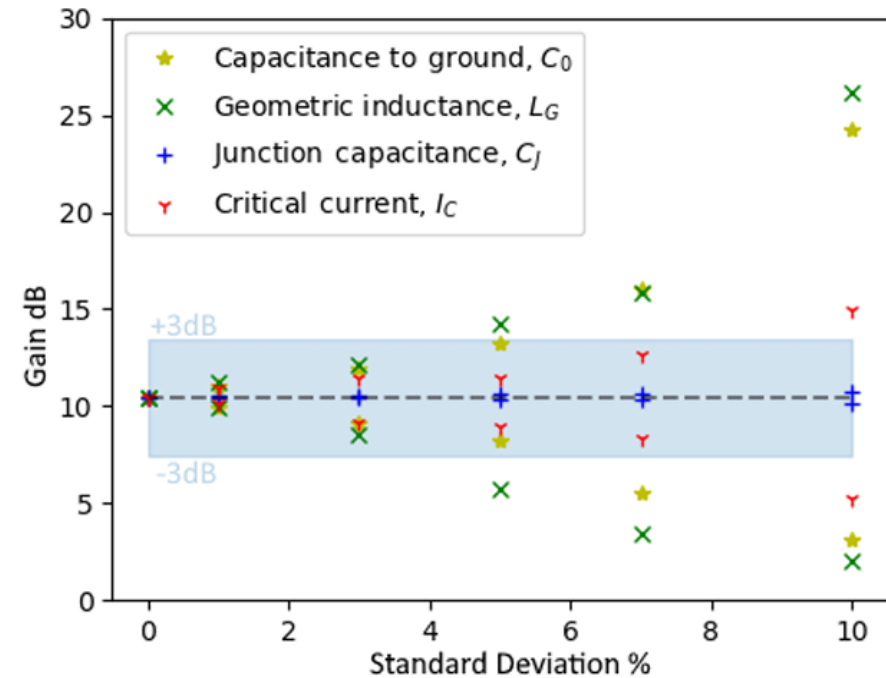


S. Pagano et al., *Development of Quantum Limited Superconducting Amplifiers for Advanced Detection*, IEEE Trans. Appl. Supercond, **32**, 4 (2022)



The role of Josephson Junction parameters spread

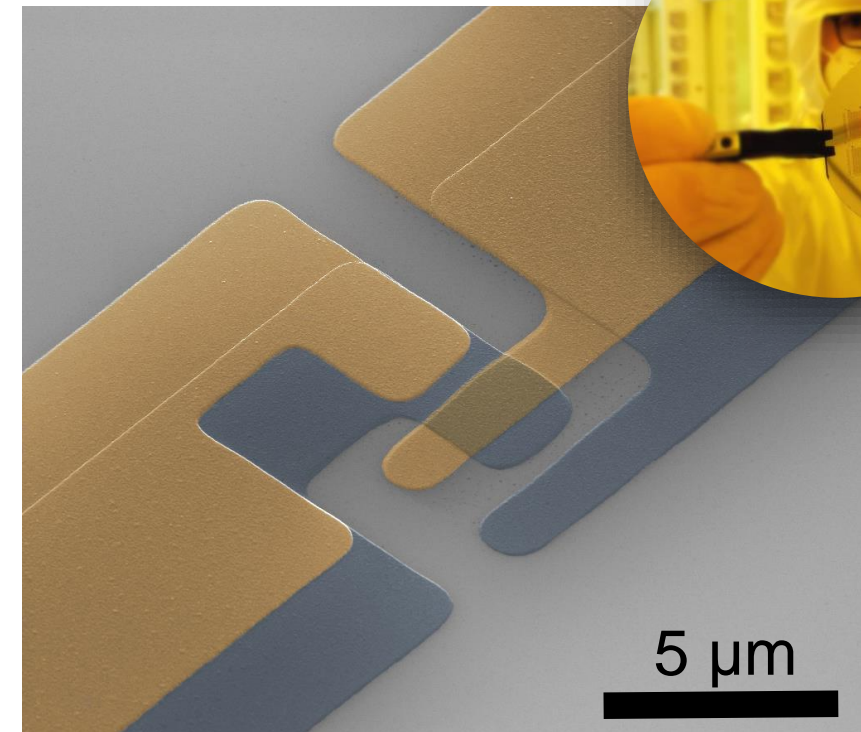
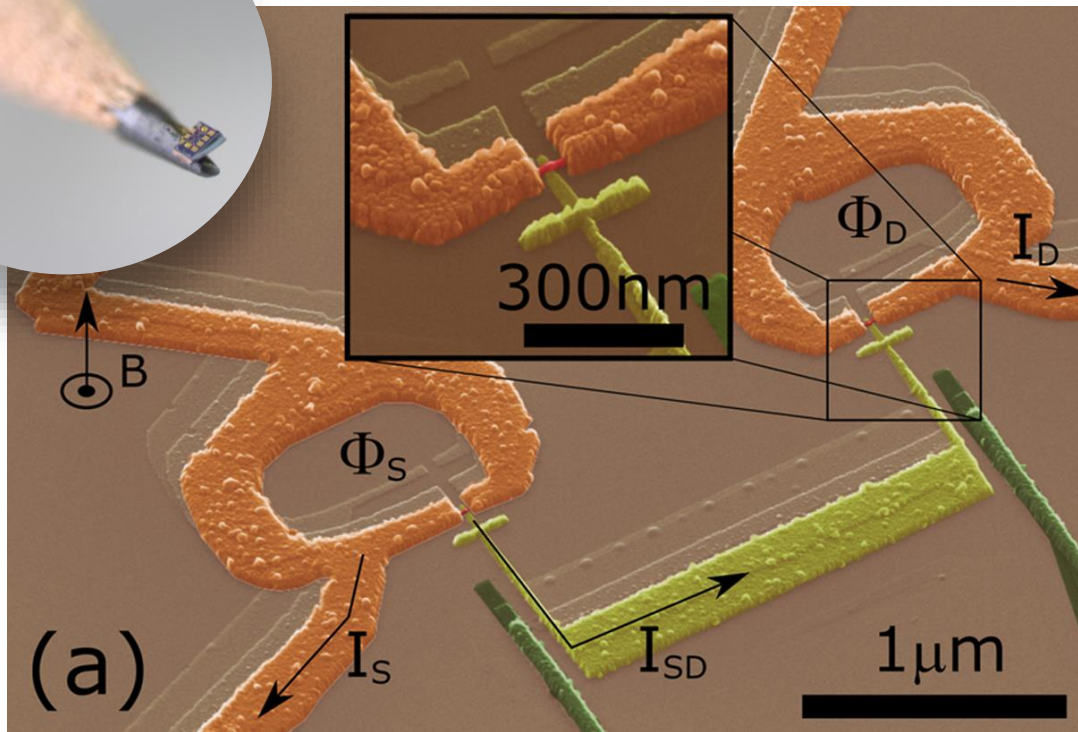
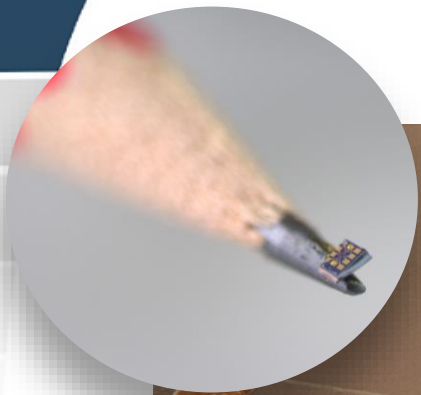
- Josephson Junction **spread** of parameters deeply affect the amplifiers performances (eg. Gain)
- Due to the exponential dependence of its properties, Josephson tunnel junctions are the **bottleneck** of the whole JTWPAs operation



The Effect of Parameter Variations on the Performance of the Josephson Travelling Wave Parametric Amplifiers, <https://arxiv.org/abs/2112.07766>

Technological challenge

Need for **reproducibility** and **stability** of Josephson Junctions on a large scale approach



E. Enrico, et al., *Single charge transport in a fully superconducting SQUSET locally tuned by self-inductance effects*, AIP Advances **12**, 055122 (2022)

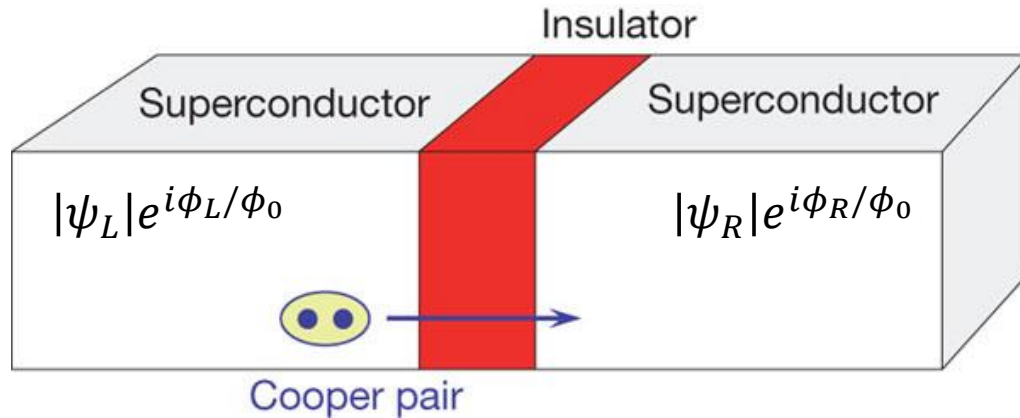
UV shadow lithography based Josephson Junction

PiQuET Cleanroom facility

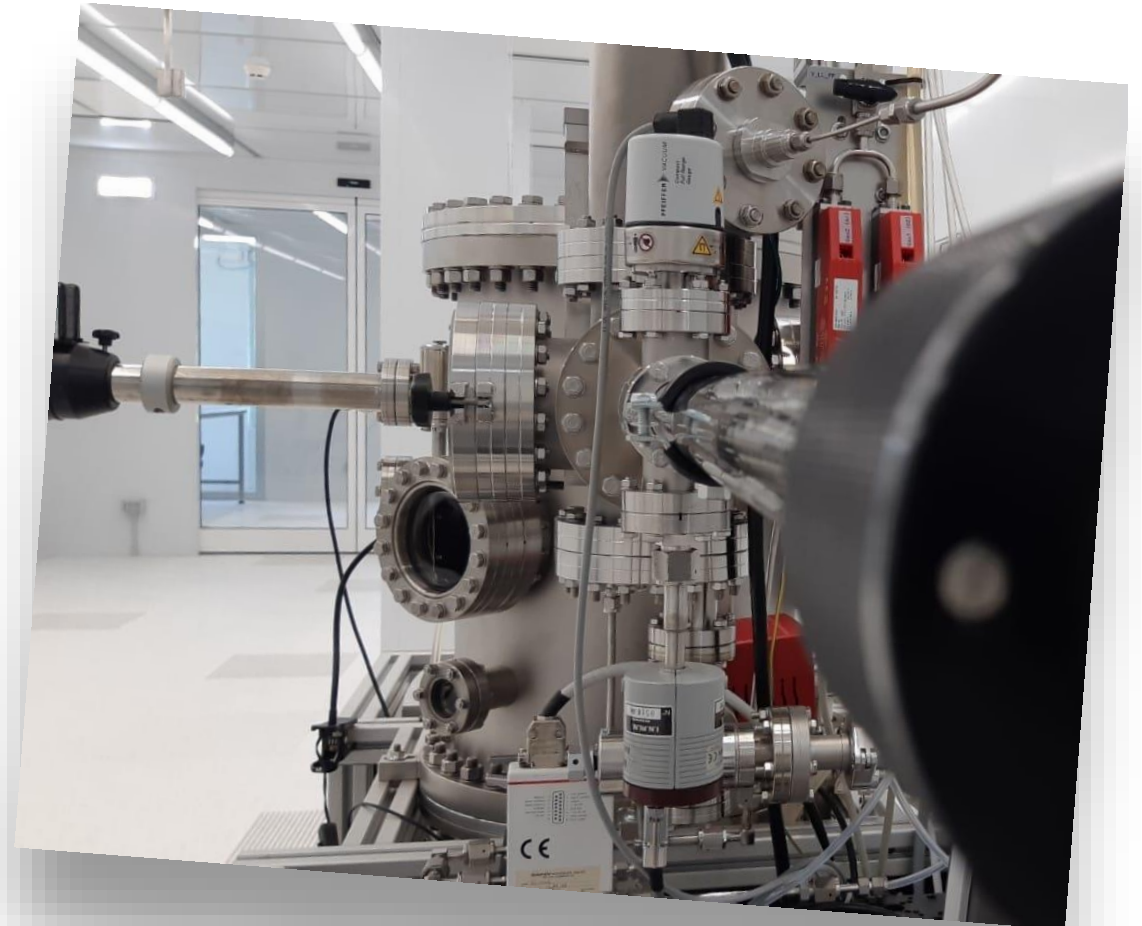
500 m² of ISO 5-6 laboratories



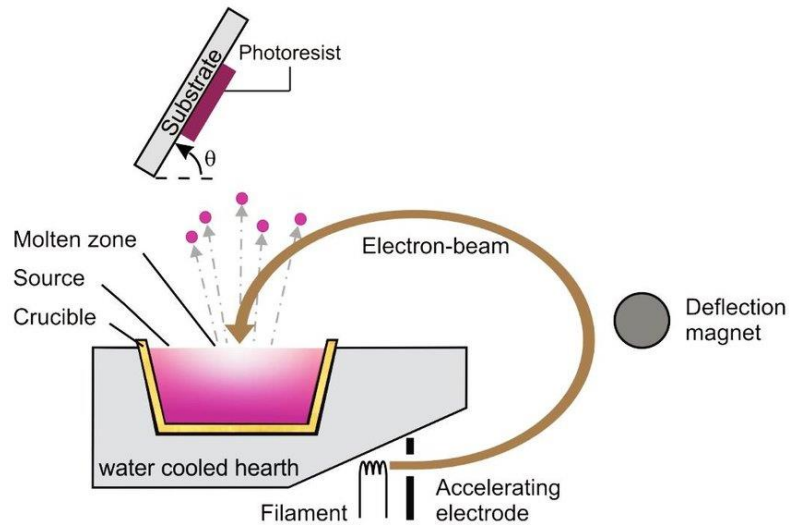
Tunnel junctions in real life



- Niobium technology
Multi-step sputtering-based process
(Nb/Al/AlO_x/Nb Technique, '80)
- Aluminum technology
Single step e-beam evap-based process
(Niemeyer-Dolan Technique, 1987)

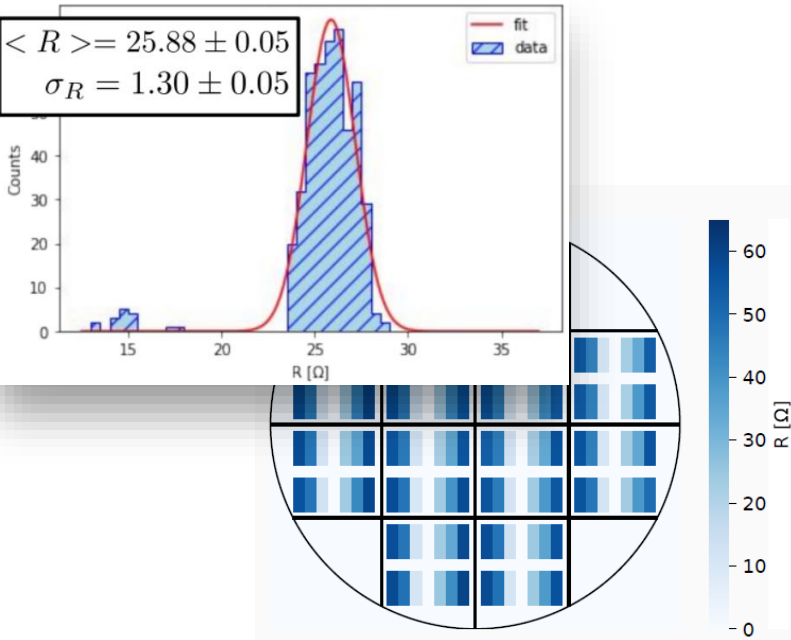
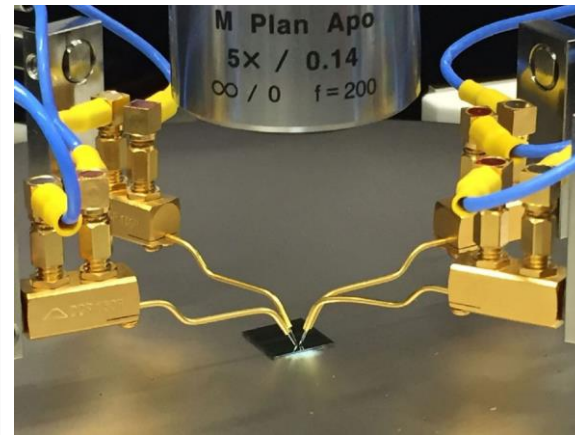
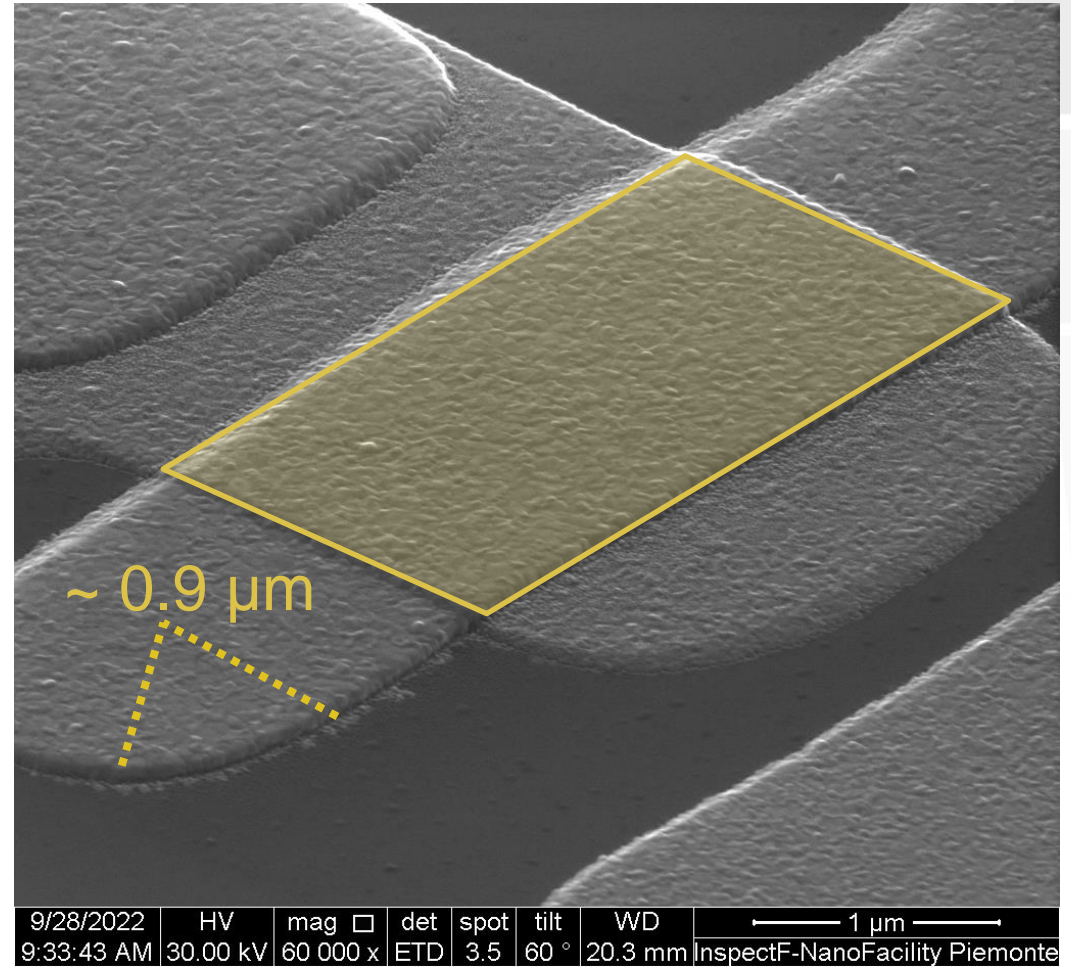


Tunnel junctions in real life



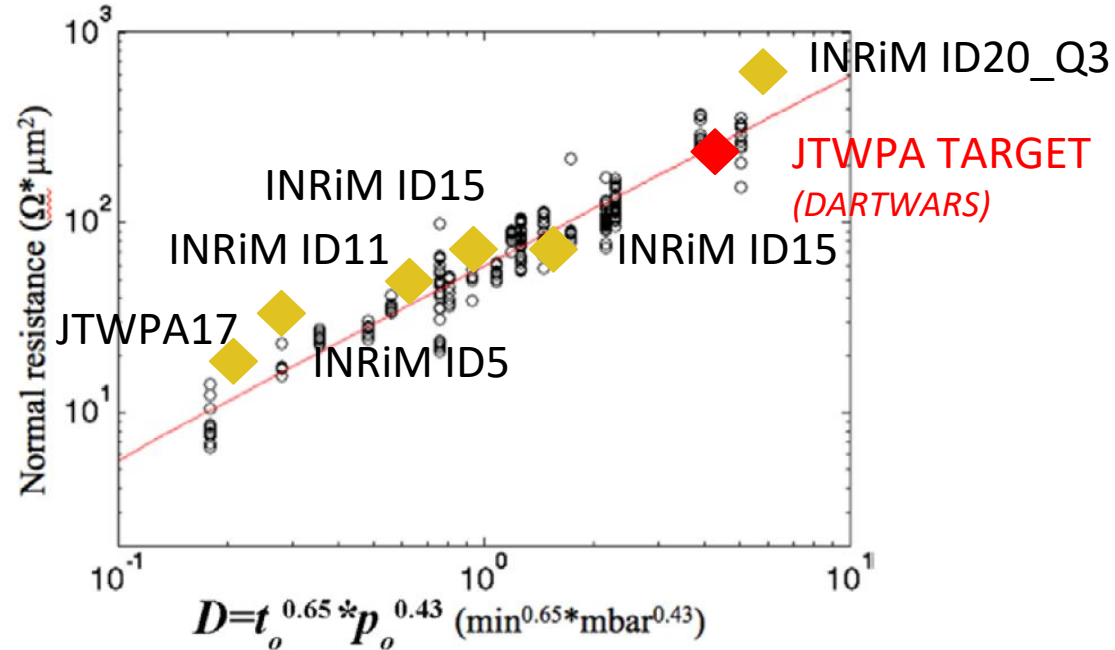
UV shadow mask lithography

- Thick and robust mask
 - compatible with O_2 ashing process
 - reduced *hillocks* formation
 - increased dielectric barrier uniformity
- Compatible with low-conductivity substrates
- Reasonable fast and reproducible process on wafer-scale
 - tested with RT semi-automatic measurements on JJs series



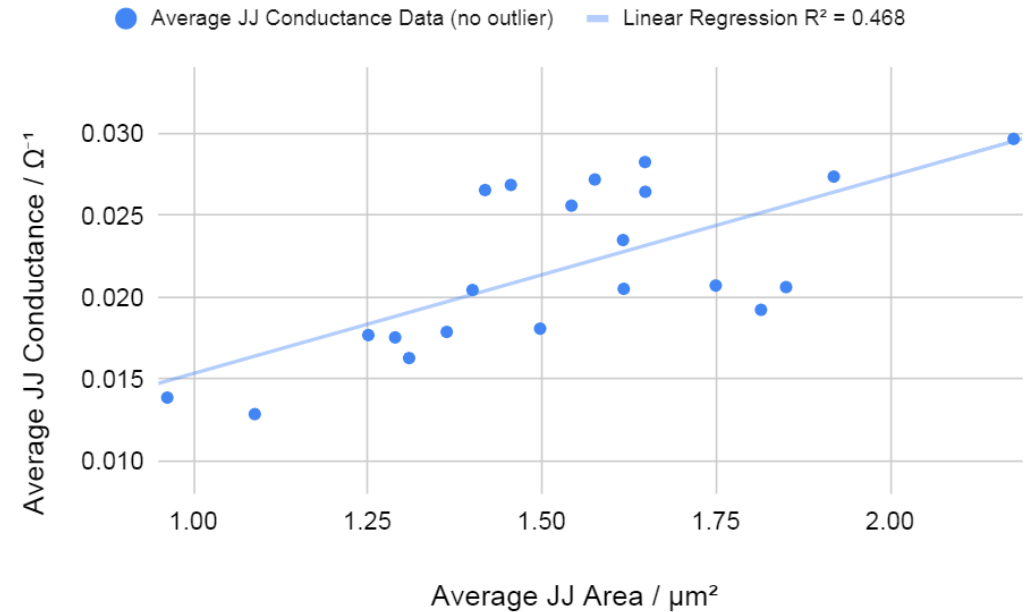
Josephson Junctions - area/oxidation interplay

Calibration points following the model presented in
L J Zeng *et al* 2015 *J. Phys. D: Appl. Phys.* **48** 395308)



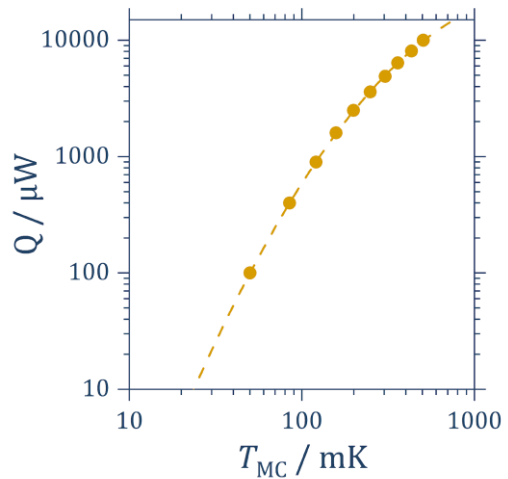
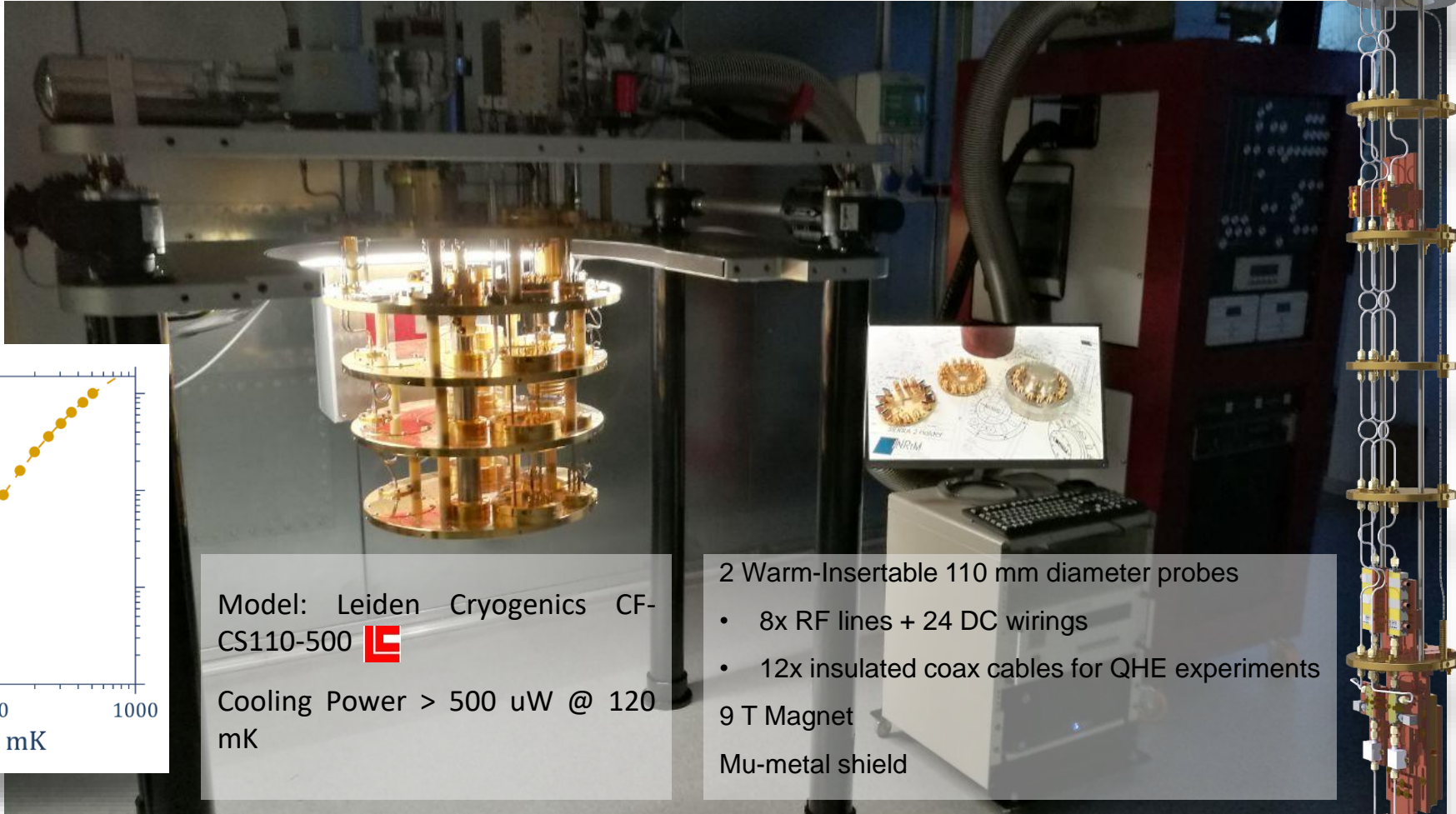
Run to run predictability and repeatability


INRiM ID15 - Area vs. Conductance correlation



On-Wafer reproducibility and homogeneity

Quantum Signals Processing Lab.



Model: Leiden Cryogenics CF-
CS110-500 

Cooling Power > 500 uW @ 120
mK

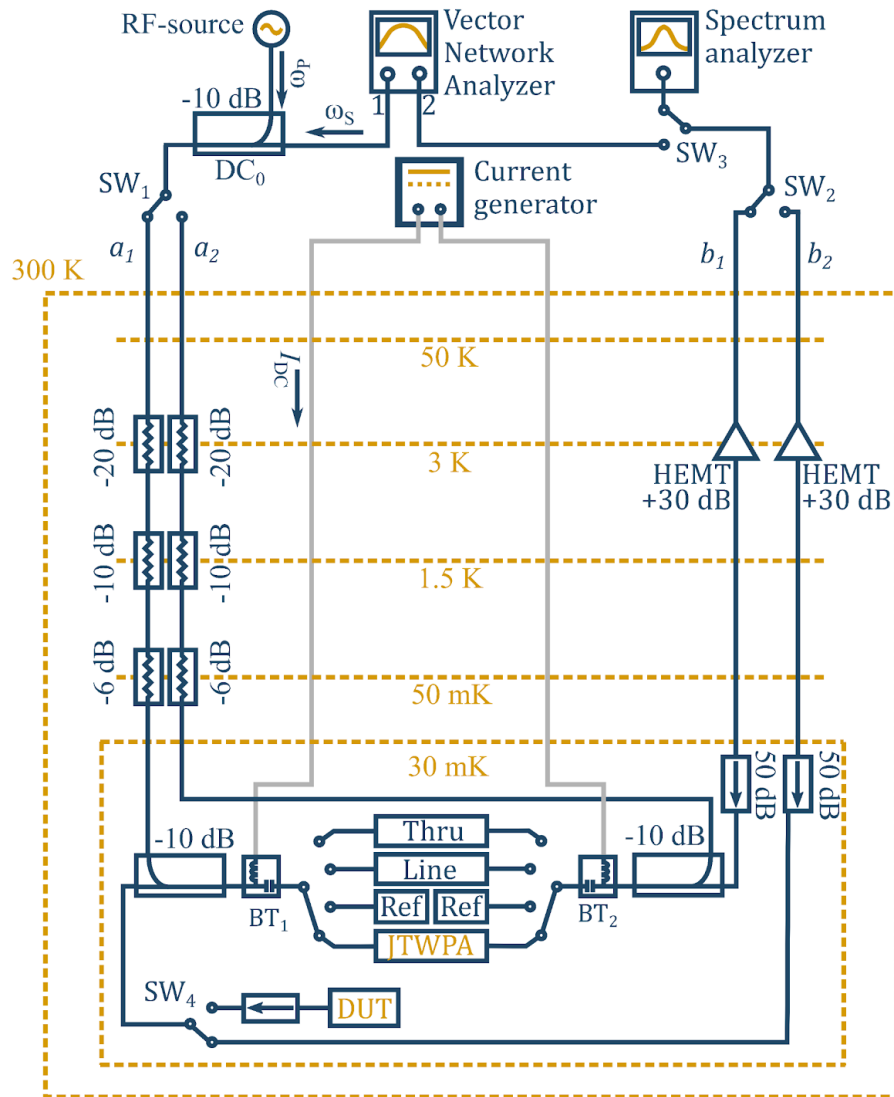
2 Warm-Insertable 110 mm diameter probes

- 8x RF lines + 24 DC wirings
- 12x insulated coax cables for QHE experiments

9 T Magnet

Mu-metal shield

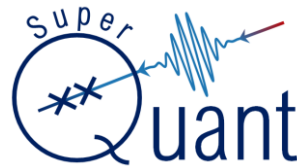
Quantum Signals Processing Lab.



Two-ports microwave **S-parameters calibration** scheme at cryogenic temperature

Uncertainty budget contributions:

- Reproducibility
- Stability
- Standards



Luca Oberto (INRiM)

Microwave metrology for superconducting quantum circuits (20FUN07 SuperQuant)

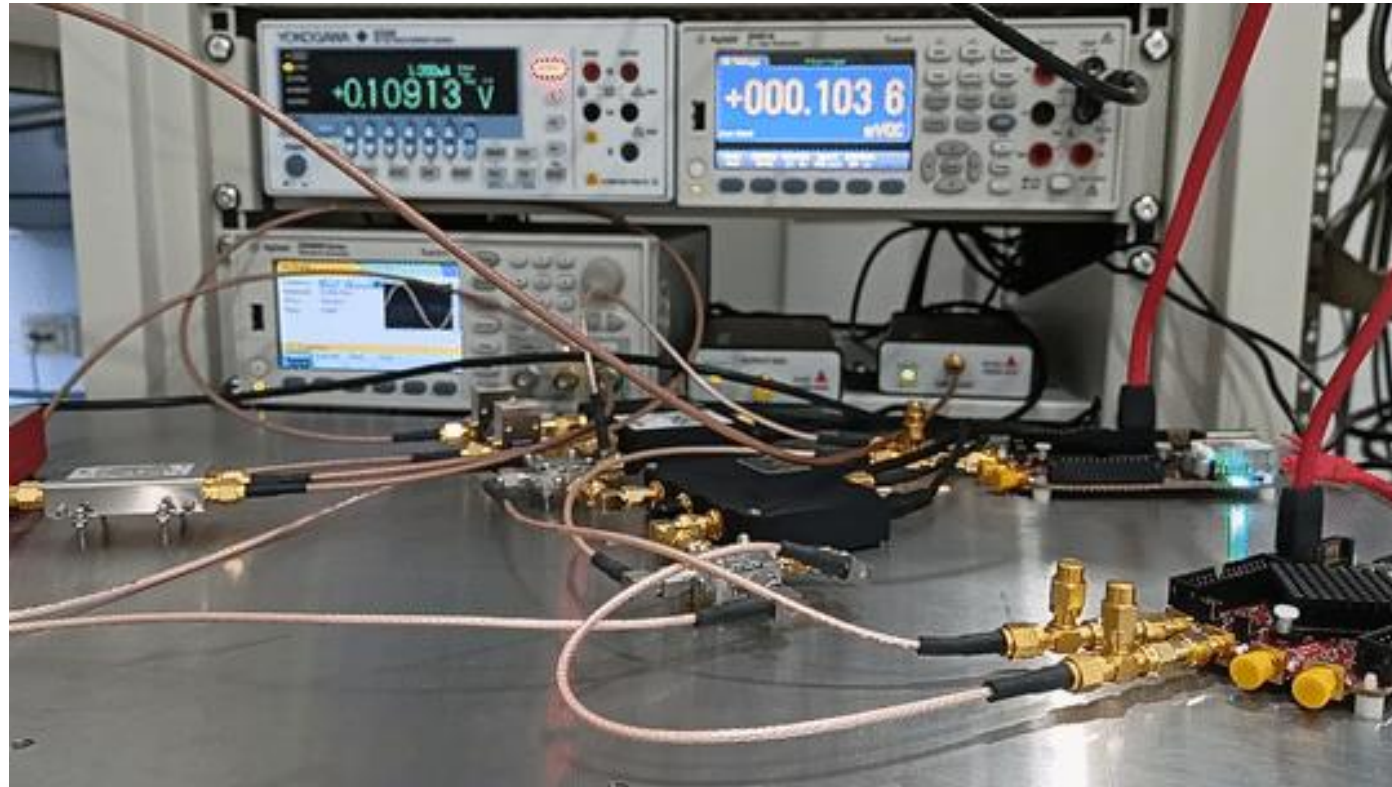


Ranzani L., Spietz L., Popovic Z., and Aumentado J., "Two-port microwave calibration at millikelvin temperatures", *Review of Scientific Instruments* **84**, 034704 (2013)



Signal processing + Control electronics

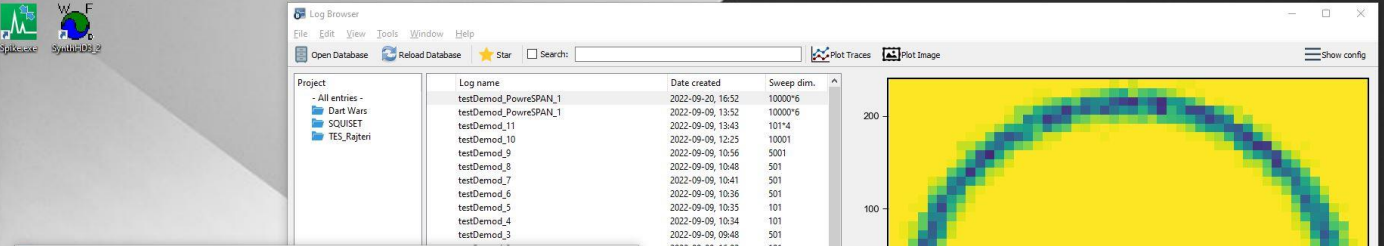
Quantum Signals Processing Laboratory



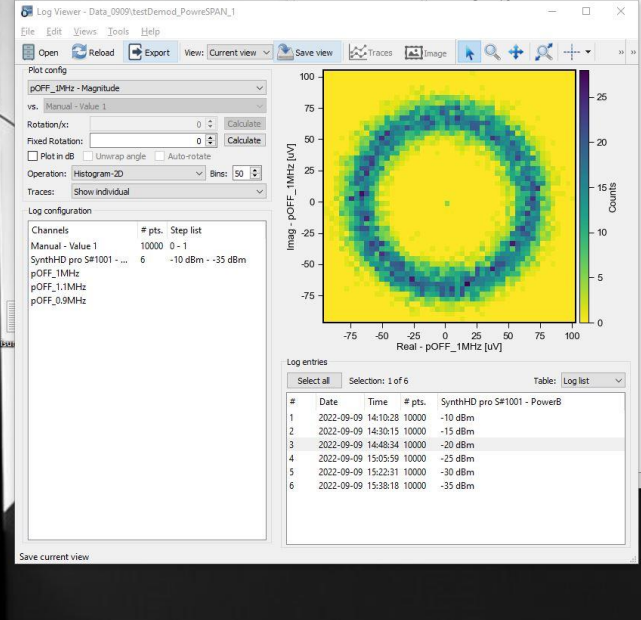
Control software

Quantum Signals Processing Laboratory

```
RedPitaya_STEMlab125-14.py x
16
17
18 class Driver(VISA_Driver):
19     """ This class implements the Agilent U2542A driver"""
20
21     def performOpen(self, options={}):
22         """Perform the operation of opening the instrument connection"""
23         # start by calling the generic VISA open to make sure we have a
24         VISA_Driver.performOpen(self, options)
25
26         self.write(':ACQ:RST')
27         self.write(':ACQ:DATA:FORMAT BIN')
28         self.write(':ACQ:DATA:UNITS VOLTS')
29         self.write(':ACQ:DEC 1')
30         self.write(':ACQ:AVG ON')
31         self.write(':ACQ:TRIG:LEV 0')
32         self.write(':ACQ:TRIG:DLY 0')
33
34     def performSetValue(self, quant, value, sweepRate=0.0, options={}):
35         """Perform the Set Value instrument operation. This function should
36         value = VISA_Driver.performSetValue(self, quant, value, sweepRate
37         return value
38
39     def performGetValue(self, quant, options={}):
40         # check type of quantity
41         if quant.name in ('RF_In1',):
42             self.write(':ACQ:START')
43             self.write(':ACQ:TRIG NOW')
44
45         while 1:
46             self.write(':ACQ:TRIG:STAT?')
47             triggStatus = self.read(None, True)
48             if triggStatus == b'TD':
49                 #self.log(triggStatus)
50                 break
51             elif triggStatus == b'TD\r\n':
52                 #self.log(triggStatus)
53
54                 self.write(':ACQ:SOUR1:DATA?')
55                 buff_byteSCARTO = self.read(None, True)
56                 #self.log(buff_byteSCARTO, 30)
57
58                 self.write(':ACQ:START')
59                 self.write(':ACQ:TRIG NOW')
60             else:
61                 self.log(triggStatus)
62
```



| Log name | Date created | Sweep dim. |
|------------------------|-------------------|------------|
| testDemod_PowereSPAN_1 | 2022-09-20, 16:52 | 10000*6 |
| testDemod_PowereSPAN_1 | 2022-09-09, 13:52 | 10000*6 |
| testDemod_11 | 2022-09-09, 13:43 | 10114 |
| testDemod_10 | 2022-09-09, 12:25 | 10001 |
| testDemod_9 | 2022-09-09, 10:56 | 5001 |
| testDemod_8 | 2022-09-09, 10:48 | 501 |
| testDemod_7 | 2022-09-09, 10:41 | 501 |
| testDemod_6 | 2022-09-09, 10:36 | 501 |
| testDemod_5 | 2022-09-09, 10:35 | 101 |
| testDemod_4 | 2022-09-09, 10:34 | 101 |
| testDemod_3 | 2022-09-09, 09:48 | 501 |
| | 2022-09-08, 16:02 | 101 |
| | 2022-09-08, 15:50 | 101 |
| | 2022-09-08, 14:56 | 101 |
| | 2022-09-08, 12:22 | 7977 |
| | 2022-09-08, 11:38 | 7977 |
| | 2022-09-08, 11:02 | 3978 |
| | 2022-07-25, 11:05 | 101 |



Log Viewer - Data_0909/testDemod_PowereSPAN_1

Plot config

pOFF_1MHz - Magnitude vs. Manual - Value 1

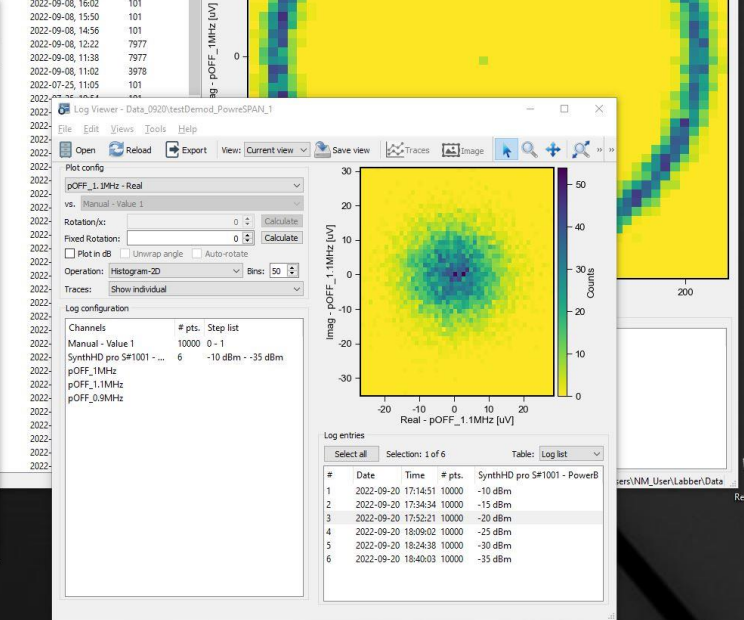
Rotation/x: 0 Calculate

Fixed Rotation/y: 0 Calculate

Plot in dB Unwrap angle Auto-rotate

Operation: Histogram-2D Bins: 50

Traces: Show individual



Log Viewer - Data_0920/testDemod_PowereSPAN_1

Plot config

pOFF_1MHz - Real vs. Manual - Value 1

Rotation/x: 0 Calculate

Fixed Rotation/y: 0 Calculate

Plot in dB Unwrap angle Auto-rotate

Operation: Histogram-2D Bins: 50

Traces: Show individual

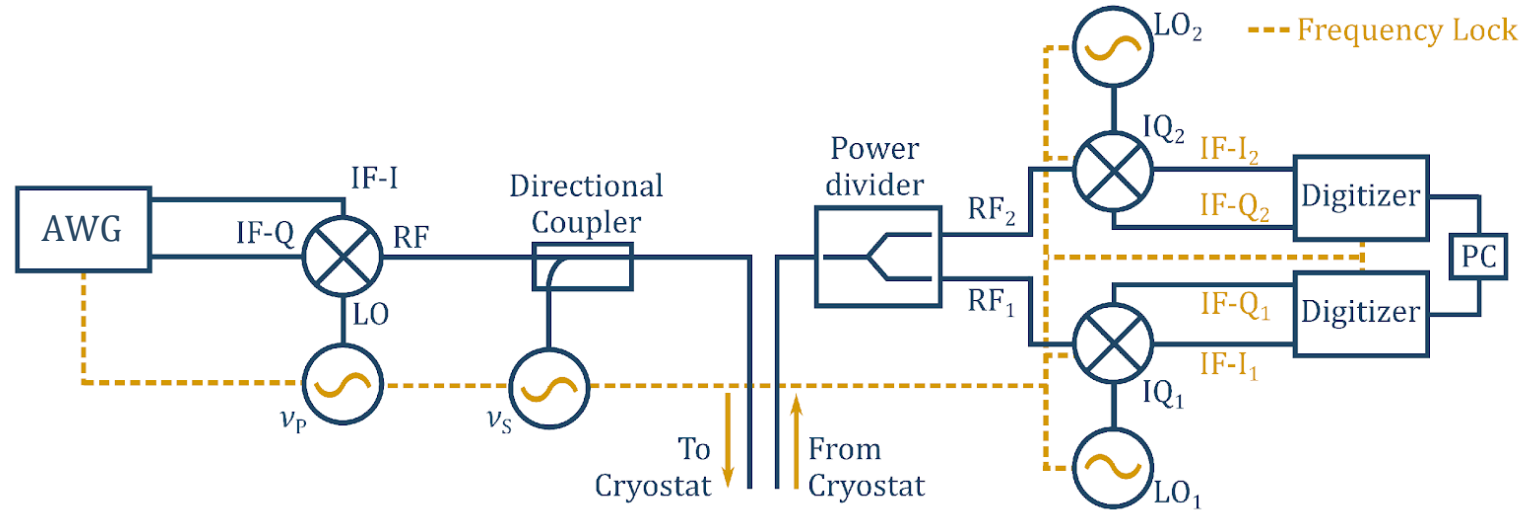
Log configuration

| Channels | # pts. | Step list |
|--------------------------|--------|-------------------|
| Manual - Value 1 | 10000 | 0 - 1 |
| SynthHD pro S#1001 - ... | 6 | -10 dBm - -35 dBm |

| # | Date | Time | # pts. | SynthHD pro S#1001 - PowerB |
|---|------------|----------|--------|-----------------------------|
| 1 | 2022-09-09 | 14:10:28 | 10000 | -10 dBm |
| 2 | 2022-09-09 | 14:30:15 | 10000 | -15 dBm |
| 3 | 2022-09-09 | 14:48:34 | 10000 | -20 dBm |
| 4 | 2022-09-09 | 15:05:59 | 10000 | -25 dBm |
| 5 | 2022-09-09 | 15:22:31 | 10000 | -30 dBm |
| 6 | 2022-09-09 | 15:38:18 | 10000 | -35 dBm |

Squeezing as a resource

Principle scheme for detecting quantum correlations in the output signals of a JTWPA



Esposito M., Ranadive A., Planat A., Leger S., Fraudet D., Jouanny V., Buisson O., Guichard W., Naud C., Aumentado J., Lecocq F., and Roch N., "Observation of Two-Mode Squeezing in a Traveling Wave Parametric Amplifier", *Phys. Rev. Lett.* **128**, 153603 (2022)



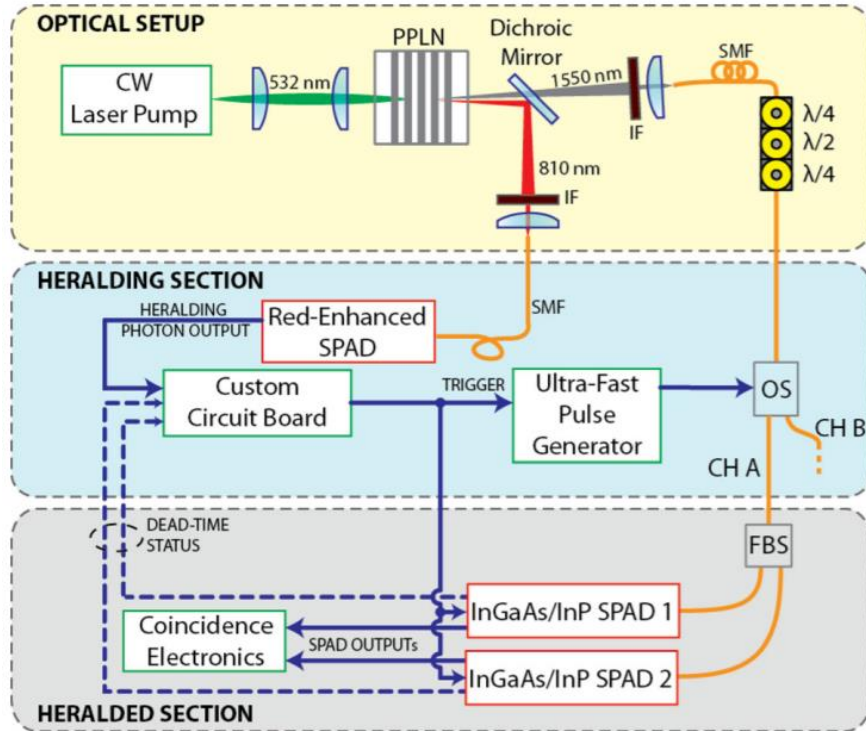
Highly sensitive detection of single microwave photons with coherent quantum network of superconducting qubits for searching galactic axions

H2020-FETOPEN-2018-2019-2020-01



Future perspectives

Single Microwave Photon Detectors (SMPD) Calibration via Heralding



SPAD analogue in the microwave regime

G. Brida et al., An extremely low-noise heralded single-photon source: A breakthrough for quantum technologies Appl. Phys. Lett. 101, 221112-1-11 (2012). doi:10.1063/1.4768288



Highly sensitive detection of single microwave photons with coherent quantum network of superconducting qubits for searching galactic axions

H2020-FETOPEN-2018-2019-2020-01





Thanks for your attention!